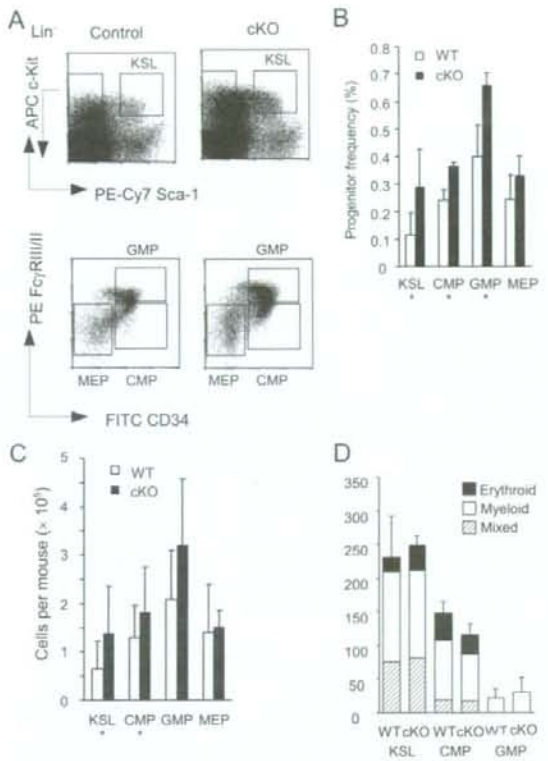

FIGURE 5. Colony-forming capacity of myeloid progenitors from cKO mice. *A*, Sorting gates of KSL, CMP, and GMP cells from control and cKO mice. *B*, Frequencies of the progenitors (KSL, CMP, GMP, and MEP for megakaryocyte/erythrocyte progenitors). *C*, Numbers of the progenitors (KSL, CMP, GMP, and MEP) per mouse calculated as products of the frequencies of the progenitors and the numbers of the total bone marrow cells per mouse. Data are also shown as mean ± SD ($n = 7$ for KSL, $n = 3$ for others) Asterisks indicate $p < 0.05$ by paired t test. *D*, Colony-forming capacity of myeloid progenitor cells. Cells sorted using the gates shown in *A* were cultured in a methylcellulose-containing medium and scored according to their morphology on day 7 of culture. ▨, mixed colonies; □, myeloid colonies, and ■, erythroid (BFU-E and CFU-E) colonies. Typical colony numbers from three independent duplicate experiments are shown. Error bars, SDs. WT, Wild type.

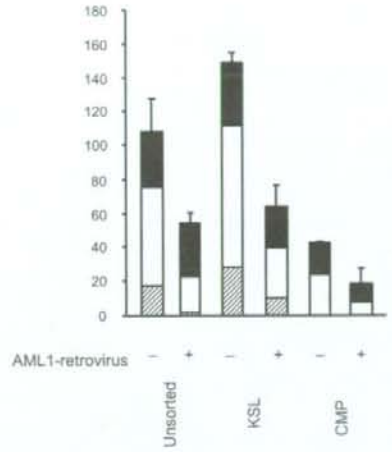

FIGURE 6. Colony-forming capacity of myeloid progenitors overexpressing AML1. Each myeloid progenitor fraction from wild-type bone marrow cells was sorted and transduced with mock or AML1-expressing retrovirus. GFP⁺ cells were sorted and cultured for 7 days in methylcellulose-containing medium supplemented with cytokines. ▨, mixed colonies; □, myeloid colonies; and ■, erythroid (BFU-E and CFU-E) colonies. Typical colony numbers from three independent duplicate experiments are shown. Error bars, SDs.

cytometry using isotypes of CD45 (Ly5) and positivity of GFP. Although all six mice showed a distinct contribution of GFP⁺ Ly5.1⁺ cells in the mock-infected group, GFP⁺ cells were detected in none of six mice transplanted with AML1-overexpressing cells (Fig. 4). These results indicated that the elevated dose of AML1 prevents hematopoietic cells from reconstituting the bone marrow of the recipient mice, again suggesting that AML1 negatively regulates hematopoietic stem cells.

Loss of AML1 causes expansion of myeloid progenitor cells without affecting their colony-forming capacity

We have previously shown that myeloid CFUs are increased when evaluated using the whole bone marrow cells of AML1-deficient mice, indicating that loss of AML1 results in an increased number of myeloid progenitors (7). These findings were consistent with another report showing that the granulocyte-macrophage progenitors (GMPs; Lin⁻Sca-1⁻c-Kit⁺CD34⁺FcγRIII/II^{high}) are increased upon deletion of AML1 in adult mice (9). Nonetheless, neutrophil counts in the peripheral blood remain unchanged in AML1-deficient mice (7). These observations allowed us to examine whether altered dosages of AML1 confer any qualitative change on the defined populations of myeloid progenitors as seen in HSCs. For this purpose, we purified each population that contains myeloid progenitors from the bone marrow and evaluated the colony-forming capacity of those cells with methylcellulose-based cultures. As is consistent with the previous report, the proportion of GMPs was elevated in the absence of AML1 (9). In addition, we found that the proportion of common myeloid progenitors (CMPs; Lin⁻Sca-1⁻c-Kit⁺CD34⁺FcγRIII/II^{low}) was also slightly but significantly elevated from poly(I:C) injection by analyzing AML1-deficient mice after 4–9 wk (Fig. 5, *A* and *B*). The total number of these progenitor cells from AML1-deficient mice was also increased, although increase in the GMP cells was not significant. These results indicate that the numbers of CMPs were negatively regulated by AML1. However, when the same number of KSL cells, CMPs, and GMPs were seeded onto methylcellulose-containing medium, colony-forming capacities were not significantly different even in the absence of AML1, indicating that loss of AML1 does not affect the quality of these progenitor populations (Fig. 5*C*). Taken together with the above findings, these results suggest that the elevated frequencies of committed progenitors in AML1-deficient bone marrow are mainly the consequences of the increased number of HSCs rather than cell-autonomous or stage-specific changes in committed progenitors.

Next, we examined the effect of overdosage of AML1 on myeloid progenitors. Unsorted cells, KSL cells, and CMPs obtained from bone marrow cells of wild-type C57BL/6J mice were transduced with mock or AML1-expressing retrovirus. Infected cells were sorted for GFP positivity and seeded onto methylcellulose-based medium. As shown in Fig. 6, KSL and CMP cells that were transduced with AML1-overexpressing retrovirus formed fewer colonies than control cells, indicating that overexpression of AML1 attenuates the proliferating capacity of these cells.

Discussion

In this article, we have found that in vivo long-term HSC activity is inversely correlated with the dosage of AML1. HSCs identified phenotypically in terms of dye efflux or cell cycle status are also increased upon deletion of AML1, which indicates that AML1 negatively regulates the number of quiescent HSCs. Increase in the quiescent fraction of HSCs in the AML1-deficient bone marrow suggests that the expansion of HSCs is not due to compensation of the differentiation block in the myeloid lineage, but the consequence of altered intrinsic transcriptional mechanisms that are physiologically regulated by AML1. Additionally, our current study shows that overexpression of AML1 in the bone marrow cells impairs hematopoietic reconstitution as well as colony-forming capacities, again suggesting that the dosage of AML1 directly regulates HSC activity.

The current observations appear to be in contrast to a previous report showing that mice that congenitally lack *AML1* in one allele contain fewer CRUs than control mice (21). This difference may depend on the time when deletion of AML1 occurs. We analyzed HSC activity immediately upon loss of AML1 by using mice that lack AML1 in an inducible fashion after birth. Mice with hemizygous levels of AML1 show aberrant distribution of definitive HSCs during embryogenesis (29), and factors like this may modify the property of HSCs in the adult stage in heterozygously AML1 knockout mice. It is known that mice that lack CBFβ, a functional partner of AML1, phenotypically recapitulate AML1 knockout mice, showing total loss of definitive hematopoiesis. A recent report using CBFβ hypomorphic mice revealed that 15% of the wild-type level of CBFβ is sufficient for emergence of definitive hematopoiesis (30). In this report, attenuated doses of CBFβ between 15 and 30% of wild type cause expansion of hematopoietic stem/progenitor cells in neonates, which return to normal when CBFβ is restored up to the hemizygous level. These facts are compatible with our findings that a reduced level of AML1 results in the expansion of HSCs after birth, although the amount of CBFβ may not linearly correlate with AML1 function. Our observation is also consistent with the earlier in vivo studies in which immature hematopoietic cells were shown to expand when they are introduced with AML1/ETO chimeric protein that represses the function of normal AML1 (15–19).

A report by another group that also analyzed conditional knockout mice of AML1 suggests that loss of AML1 does not affect long-term HSC activity, although they do not directly estimate the frequency of HSCs in the bone marrow (9). They also reported that AML1-deficient HSCs show impaired chimerism in the competitive transplantation assays. In this respect, we previously showed that the long-term myeloid-repopulating capacity of AML1-deficient cells, as measured by donor cell chimerism in the peripheral blood at 3 mo, is no better than that of control cells in the competitive transplantation assays (7). Therefore, subtle block of myeloid differentiation, which cannot be detected in in vitro colony-forming assays, may exist and impair myeloid cell reconstitution in the absence of AML1. In addition, given that CRUs in the AML1-deficient bone marrow are ~10 times higher compared with the control bone marrow, mean activity of stem cells, which is indicated as repopulating units per CRU (31), may be diminished in the absence of AML1. Another difference between the two studies is that they did not detect any increase in the proportion of CMPs in the AML1-deficient bone marrow as is contrasted with our results. This may be due to the difference in the periods from AML1 deletion to the analysis (4–9 wk vs 17–39 wk), although there are other possibilities.

Given that loss of AML1 causes expansion of HSCs in adult bone marrow, genetic aberrations involving AML1 found in human leukemias may also promote expansion of leukemic stem cells by inhibiting AML1 function, although it remains yet to be determined whether normal and leukemic stem cells are maintained through similar molecular mechanisms. Elucidation of such mechanisms would be a clue to a more precise understanding of normal hematopoiesis and hematological malignancies. Analyses on mutant mice have shown that various genes, including those for transcription factors, cell surface ligands, their cognate receptors, cell cycle proteins, and molecules involved in signal transduction, control the HSC pool size (reviewed in Ref. 32). AML1 is documented to regulate the expression of target genes that act mainly in committed hematopoietic cells, such as IL-3, myeloperoxidase, neutrophil elastase, M-CSF receptor, GM-CSF, TCRs (reviewed in Ref. 33), Ig α-chain (34–36), and λ5 (37). In contrast, little is known about candidates for transcriptional targets of AML1 in adult HSCs. The regulatory mechanism of transcription through which AML1 controls the size of the HSC pool remains an unanswered question that should be elucidated in future studies.

In this study, we have explicitly shown that AML1 negatively regulates the number of HSCs in the quiescent state in adult hematopoiesis. Expansion of the immature hematopoietic cells caused by disruption of AML1 function may be involved in the pathogenesis of hematological malignancies associated with altered AML1 function.

Acknowledgments

We thank H. Nakauchi for the retrovirus vector and C57BL/6-Ly-5.1-congenic mice, R. Kühn and J. Takeda for the *Mx-cre*-transgenic mice, N. Watanabe and T. Kitamura for the protocol for retroviral transduction, and Y. Sawamoto and Y. Shimamura for technical assistance.

Disclosures

The authors have no financial conflict of interest.

References

1. Dzierzak, E., and A. Medvinsky. 1995. Mouse embryonic hematopoiesis. *Trends Genet.* 11: 359–366.
2. Medvinsky, A., and E. Dzierzak. 1996. Definitive hematopoiesis is autonomously initiated by the AGM region. *Cell* 86: 897–906.
3. Muller, A. M., A. Medvinsky, J. Strouboulis, F. Grosveld, and E. Dzierzak. 1994. Development of hematopoietic stem cell activity in the mouse embryo. *Immunity* 1: 291–301.
4. Miyoshi, H., K. Shimizu, T. Kozu, N. Maseki, Y. Kaneko, and M. Ohki. 1991. t(8;21) breakpoints on chromosome 21 in acute myeloid leukemia are clustered within a limited region of a single gene, AML1. *Proc. Natl. Acad. Sci. USA* 88: 10431–10434.
5. Okuda, T., J. van Deursen, S. W. Hiebert, G. Grosveld, and J. R. Downing. 1996. AML1, the target of multiple chromosomal translocations in human leukemia, is essential for normal fetal liver hematopoiesis. *Cell* 84: 321–330.
6. Wang, Q., T. Stacy, M. Binder, M. Marin-Padilla, A. H. Sharpe, and N. A. Speck. 1996. Disruption of the Cbfa2 gene causes necrosis and hemorrhaging in the central nervous system and blocks definitive hematopoiesis. *Proc. Natl. Acad. Sci. USA* 93: 3444–3449.
7. Ichikawa, M., T. Asai, T. Saito, S. Seo, I. Yamazaki, T. Yamagata, K. Mitani, S. Chiba, S. Ogawa, M. Kurokawa, and H. Hirai. 2004. AML-1 is required for megakaryocytic maturation and lymphocytic differentiation, but not for maintenance of hematopoietic stem cells in adult hematopoiesis. *Nat. Med.* 10: 299–304.
8. Putz, G., A. Rosner, I. Nuesslein, N. Schmitz, and F. Buchholz. 2006. AML1 deletion in adult mice causes splenomegaly and lymphomas. *Oncogene* 25: 929–939.
9. Growney, J. D., H. Shigematsu, Z. Li, B. H. Lee, J. Adelsperger, R. Rowan, D. P. Curley, J. L. Kutok, K. Akashi, I. R. Williams, et al. 2005. Loss of Runx1 perturbs adult hematopoiesis and is associated with a myeloproliferative phenotype. *Blood* 106: 494–504.
10. Mikkola, H. K., J. Klintman, H. Yang, H. Hock, T. M. Schlaeger, Y. Fujiwara, and S. H. Orkin. 2003. Haematopoietic stem cells retain long-term repopulating activity and multipotency in the absence of stem-cell leukaemia SCL/tal-1 gene. *Nature* 421: 547–551.
11. Radtke, F., A. Wilson, G. Stark, M. Bauer, J. van Meerwijk, H. R. MacDonald, and M. Aguet. 1999. Deficient T cell fate specification in mice with an induced inactivation of Notch1. *Immunity* 10: 547–558.

12. Osato, M., N. Asou, E. Abdalla, K. Hoshino, H. Yamasaki, T. Okubo, H. Suzushima, K. Takatsuki, T. Kanno, K. Shigesada, and Y. Ito. 1999. Biallelic and heterozygous point mutations in the runt domain of the AML1/PEBP2αB gene associated with myeloblastic leukemias. *Blood* 93: 1817–1824.
13. Imai, Y., M. Kurokawa, K. Izutsu, A. Hangaishi, K. Takeuchi, K. Maki, S. Ogawa, S. Chiba, K. Mitani, and H. Hirai. 2000. Mutations of the AML1 gene in myelodysplastic syndrome and their functional implications in leukemogenesis. *Blood* 96: 3154–3160.
14. Song, W. J., M. G. Sullivan, R. D. Legare, S. Hutchings, X. Tan, D. Kufrin, J. Ratajczak, I. C. Resende, C. Haworth, R. Hock, et al. 1999. Haploinsufficiency of CBFA2 causes familial thrombocytopenia with propensity to develop acute myelogenous leukaemia. *Nat. Genet.* 23: 166–175.
15. de Guzman, C. G., A. J. Warren, Z. Zhang, L. Gartland, P. Erickson, H. Drabkin, S. W. Hiebert, and C. A. Klug. 2002. Hematopoietic stem cell expansion and distinct myeloid developmental abnormalities in a murine model of the AML1-ETO translocation. *Mol. Cell. Biol.* 22: 5506–5517.
16. Fenske, T. S., G. Pengue, V. Mathews, P. T. Hanson, S. E. Hamm, N. Riaz, and T. A. Graubert. 2004. Stem cell expression of the AML1/ETO fusion protein induces a myeloproliferative disorder in mice. *Proc. Natl. Acad. Sci. USA* 101: 15184–15189.
17. Schwieger, M., J. Lohler, J. Friel, M. Scheller, I. Horak, and C. Stocking. 2002. AML1-ETO inhibits maturation of multiple lymphohematopoietic lineages and induces myeloblast transformation in synergy with ICSBP deficiency. *J. Exp. Med.* 196: 1227–1240.
18. Yuan, Y., L. Zhou, T. Miyamoto, H. Iwasaki, N. Harakawa, C. J. Hetherington, S. A. Burel, E. Lagasse, I. L. Weissman, K. Akashi, and D. E. Zhang. 2001. AML1-ETO expression is directly involved in the development of acute myeloid leukemia in the presence of additional mutations. *Proc. Natl. Acad. Sci. USA* 98: 10398–10403.
19. Higuchi, M., D. O'Brien, P. Kumaravelu, N. Lenny, E. J. Yeoh, and J. R. Downing. 2002. Expression of a conditional AML1-ETO oncogene bypasses embryonic lethality and establishes a murine model of human t(8;21) acute myeloid leukemia. *Cancer Cell* 1: 63–74.
20. Yan, M., E. Kanbe, L. F. Peterson, A. Boyapati, Y. Miao, Y. Wang, I. M. Chen, Z. Chen, J. D. Rowley, C. L. Willman, and D. E. Zhang. 2006. A previously unidentified alternatively spliced isoform of t(8;21) transcript promotes leukemogenesis. *Nat. Med.* 12: 945–949.
21. Sun, W., and J. R. Downing. 2004. Haploinsufficiency of AML1 results in a decrease in the number of LTR-HSCs while simultaneously inducing an increase in more mature progenitors. *Blood* 104: 3565–3572.
22. Kuhn, R., F. Schwenk, M. Aguet, and K. Rajewsky. 1995. Inducible gene targeting in mice. *Science* 269: 1427–1429.
23. Muskiewicz, K. R., N. Y. Frank, A. F. Flint, and E. Gussoni. 2005. Myogenic potential of muscle side and main population cells after intravenous injection into sub-lethally irradiated mdx mice. *J. Histochem. Cytochem.* 53: 861–873.
24. Goodell, M. A., K. Brose, G. Paradis, A. S. Conner, and R. C. Mulligan. 1996. Isolation and functional properties of murine hematopoietic stem cells that are replicating in vivo. *J. Exp. Med.* 183: 1797–1806.
25. Arai, F., A. Hirao, M. Ohmura, H. Sato, S. Matsuoka, K. Takubo, K. Ito, G. Y. Koh, and T. Suda. 2004. Tie2/angiopoietin-1 signaling regulates hematopoietic stem cell quiescence in the bone marrow niche. *Cell* 118: 149–161.
26. Matsuzaki, Y., K. Kinjo, R. C. Mulligan, and H. Okano. 2004. Unexpectedly efficient homing capacity of purified murine hematopoietic stem cells. *Immunity* 20: 87–93.
27. Kawazu, M., T. Asai, M. Ichikawa, G. Yamamoto, T. Saito, S. Goyama, K. Mitani, K. Miyazono, S. Chiba, S. Ogawa, et al. 2005. Functional domains of Runx1 are differentially required for CD4 repression: TCRβ expression, and CD4/8 double-negative to CD4/8 double-positive transition in thymocyte development. *J. Immunol.* 174: 3526–3533.
28. Szilvassy, S. J., R. K. Humphries, P. M. Lansdorp, A. C. Eaves, and C. J. Eaves. 1990. Quantitative assay for totipotent reconstituting hematopoietic stem cells by a competitive repopulation strategy. *Proc. Natl. Acad. Sci. USA* 87: 8736–8740.
29. Cai, Z., M. de Bruijn, X. Ma, B. Dortland, T. Luteijn, R. J. Downing, and E. Dzierzak. 2000. Haploinsufficiency of AML1 affects the temporal and spatial generation of hematopoietic stem cells in the mouse embryo. *Immunity* 13: 423–431.
30. Talebian, L., Z. Li, Y. Guo, J. Gaudet, M. E. Speck, D. Sugiyama, P. Kaur, W. S. Pear, I. Maillard, and N. A. Speck. 2006. T lymphoid, megakaryocyte, and granulocyte development are sensitive to decreases in CBFβ dosage. *Blood* 109: 11–21.
31. Ema, H., and H. Nakauchi. 2000. Expansion of hematopoietic stem cells in the developing liver of a mouse embryo. *Blood* 95: 2284–2288.
32. Wilson, A., and A. Trumpp. 2006. Bone-marrow haematopoietic-stem-cell niches. *Nat. Rev. Immunol.* 6: 93–106.
33. Lutterbach, B., and S. W. Hiebert. 2000. Role of the transcription factor AML-1 in acute leukemia and hematopoietic differentiation. *Gene* 245: 223–235.
34. Hanai, J., L. F. Chen, T. Kanno, N. Ohtani-Fujita, W. Y. Kim, W. H. Guo, T. Imamura, Y. Ishidou, M. Fukuchi, M. J. Shi, et al. 1999. Interaction and functional cooperation of PEBP2/CBF with Smads: synergistic induction of the immunoglobulin germline Cα promoter. *J. Biol. Chem.* 274: 31577–31582.
35. Pardali, E., X. Q. Xie, P. Tsapogas, S. Itoh, K. Arvanitidis, C. H. Heldin, P. ten Dijke, T. Grundstrom, and P. Sideras. 2000. Smad and AML proteins synergistically confer transforming growth factor β1 responsiveness to human germ-line IgA genes. *J. Biol. Chem.* 275: 3552–3560.
36. Zhang, Y., and R. Derynck. 2000. Transcriptional regulation of the transforming growth factor-β-inducible mouse germ line Ig α constant region gene by functional cooperation of Smad, CREB, and AML family members. *J. Biol. Chem.* 275: 16979–16985.
37. Martensson, A., X. Q. Xie, C. Persson, M. Holm, T. Grundstrom, and I. L. Martensson. 2001. PEBP2 and c-myb sites crucial for λ5 core enhancer activity in pre-B cells. *Eur. J. Immunol.* 31: 3165–3174.

Oncogene (2008) 27, 6023–6033

www.nature.com/onc

ORIGINAL ARTICLE

v-Src oncogene product increases sphingosine kinase 1 expression through mRNA stabilization: alteration of AU-rich element-binding proteins

S Sobue[1], M Murakami[1], Y Banno[2], H Ito[1], A Kimura[1], S Gao[1], A Furuhata[1], A Takagi[1], T Kojima[1], M Suzuki[3], Y Nozawa[4] and T Murate[1]

[1]*Department of Medical Technology, Nagoya University Graduate School of Health Sciences, Nagoya, Japan;* [2]*Department of Biochemistry, Gifu University Graduate School of Medicine, Gifu, Japan;* [3]*Division of Molecular Carcinogenesis, Nagoya University Graduate School of Medicine, Nagoya, Japan and* [4]*Gifu International Institute of Biotechnology, Kakamigahara, Japan*

Sphingosine kinase 1 (SPHK1) is overexpressed in solid tumors and leukemia. However, the mechanism of SPHK1 overexpression by oncogenes has not been defined. We found that *v-Src*-transformed NIH3T3 cells showed a high *SPHK1* mRNA, SPHK1 protein and SPHK enzyme activity. siRNA of *SPHK1* inhibited the growth of *v-Src*-NIH3T3, suggesting the involvement of SPHK1 in *v-Src*-induced oncogenesis. *v-Src*-NIH3T3 showed activations of protein kinase C-α, signal transducers and activators of transcription 3 and c-Jun NH_2-terminal kinase. Their inhibition suppressed SPHK1 expression in *v-Src*-NIH3T3, whereas their overexpression increased *SPHK1* mRNA in NIH3T3. Unexpectedly, the nuclear run-on assay and the promoter analysis using 5′-promoter region of mouse *SPHK1* did not show any significant difference between mock- and *v-Src*-NIH3T3. Furthermore, the half-life of *SPHK1* mRNA in mock-NIH3T3 was nearly 15 min, whereas that of *v-Src*-NIH3T3 was much longer. Examination of two AU-rich region-binding proteins, AUF1 and HuR, that regulate mRNA decay reciprocally, showed decreased total AUF1 protein associated with increased tyrosine-phosphorylated form and increased serine-phosphorylated HuR protein in *v-Src*-NIH3T3. Modulation of AUF1 and HuR by their overexpression or siRNA revealed that SPHK1 mRNA in *v-Src*- and mock-NIH3T3 was regulated reciprocally by these factors. Our results showed, for the first time, a novel mechanism of *v-Src*-induced *SPHK1* overexpression.
Oncogene (2008) **27,** 6023–6033; doi:10.1038/onc.2008.198; published online 23 June 2008

Keywords: *v-Src*; sphingosine kinase 1; gene expression; mRNA half-life; AUF1; HuR

Correspondence: Dr T Murate, Department of Medical Technology, Nagoya University School of Health Sciences, Daiko Minami 1-1-20, Higashi-ku, Nagoya 466-8673, Japan.
E-mail: murate@met.nagoya-u.ac.jp
Received 4 February 2008; revised 1 May 2008; accepted 15 May 2008; published online 23 June 2008

Introduction

Sphingosine kinase (SPHK) is a key enzyme in the sphingolipid metabolic pathway as it forms an essential checkpoint that regulates the relative levels of sphingosine 1-phosphate (S1P), sphingosine and ceramide. SPHK mediates the growth response by several growth stimulation signals (Taha *et al.*, 2006). S1P is a bioactive sphingolipid metabolite that is produced by SPHK, and has been implicated in many biological processes such as cell survival, cell proliferation, angiogenesis and cell migration. S1P can function intracellularly as a second messenger or activate signaling through S1P receptors in an autocrine and/or paracrine fashion (Alvarez *et al.*, 2007).

We previously reported that *SPHK1* mRNA was stimulated with nerve growth factor (NGF) or phorbol ester (Nakade *et al.*, 2003; Sobue *et al.*, 2005). Furthermore, SPHK1 overexpression enhances the growth of cells even without extracellular stimulation (Olivera *et al.*, 1999). These results suggest an oncogenic role of SPHK1 in cancer. Kawamori *et al.* (2006) reported that *SPHK1* mRNA and protein levels were increased in human colon cancer, and we recently observed an increased *SPHK1* mRNA in acute leukemia and myelodysplastic syndromes (Sobue *et al.*, 2006). An inhibitor of SPHK is antiproliferative and proapoptotic to several tumor cell lines (French *et al.*, 2003). We as well as others have shown that the inhibition of SPHK1 activity enhances the chemosensitivity of cancer cells (Bektas *et al.*, 2005; Akao *et al.*, 2006; Bonhoure *et al.*, 2006).

However, direct analyses of the relationship between oncogene and SPHK1 expression are rare. Xia *et al.* (2000) reported mutated *Ras* as a stimulator of SPHK, but its underlying mechanism has not been extensively studied. Src and Src-family protein kinases (SFKs) are proto-oncogenes that play key roles in cell morphology, motility, proliferation and survival. *v-Src* is encoded by the chicken oncogene of Rous sarcoma virus, and *c-Src*, encoded by a physiological gene, is the first example of the proto-oncogenes. Activation of SFKs allows phosphorylation of specific substrates. Growth stimulation by *v-Src* requires activation of MEK/ERK (mitogen-activated protein kinase kinase/extracellular regulated kinase) and other signaling pathways (Frame, 2004).

v-Src, but not *c-Src*, transforms NIH3T3 cells. However, like *v-Src*, activated mutants of *c-Src* can

transform cells in culture and induce tumors in chickens. Recently, overexpression of *c-Src* was observed in many human tumors (Dehm *et al*., 2001; Dehm and Bonham, 2004). Transformation due to *v-Src* probably results from perturbation of normal growth or a developmental regulatory pathway mediated by *c-Src*. Analysis of the mechanism of *SPHK1* overexpression by oncogenes is important to evaluate their clinical significance because SPHK inhibitors could be expected to show promise as valuable reagents to treat solid tumors and leukemia.

In this study, we analysed SPHK expression using *v-Src*-transformed NIH3T3 cells and found a novel mechanism of *SPHK1* mRNA increase based on its stabilization. We further examined the involvement of AU-rich region (AUR)-binding proteins (AUBPs), AUF1 and HuR (Kloss *et al*., 2004; Lal *et al*., 2004; Raineri *et al*., 2004), regulating mRNA decay in the opposite direction. The role of the aberrant expression of AUBPs in *v-Src*-NIH3T3 in *SPHK1* mRNA stabilization and the signaling pathway, which starts from *v-Src* and ends at the binding of AUBPs to 3′ UTR of *SPHK1* mRNA, were discussed.

Results

v-Src-*transfected cells showed both increased* SPHK1 *mRNA and enzyme activity*

SPHK1 protein levels of stable transfectants of mock-, dominant-negative (DN) *c-Src*-, *v-Src*- and mutated *H-Ras*-NIH3T3 are shown in Figure 1a. Overexpression of Src or Ras of respective transformants was also confirmed. *DN-c-Src*-NIH3T3 also showed an increase of Src protein. Although Xia *et al*. (2000) reported the increased SPHK enzyme activity in mutated *H-Ras*-transfected NIH3T3 cells, our repeated trial of mutated *H-Ras* transfection into NIH3T3 cells showed a marginal SPHK1 protein overexpression and enzyme activity, although high SPHK1 protein levels were constantly observed in *v-Src*-transformed NIH3T3. Transient transfection experiments of mutated *K-Ras*, mutated *H-Ras* and *v-Src* showed similar results (data not shown).

SPHK enzyme activity shown in Figure 1b also demonstrates its increase in *v-Src*-NIH3T3 and a mild increase in mutated *H-Ras*-NIH3T3. Figure 1c shows *SPHK1* mRNA measured by real-time reverse transcriptase (RT)–PCR. Both *v-Src* and mutated *H-Ras* increased *SPHK1* mRNA. The increase of *SPHK1* mRNA in *v-Src*-NIH3T3 is also much higher than that of mutated *H-Ras*-NIH3T3. In addition, DN-*c-Src*-NIH3T3 showed a very low *SPHK1* mRNA, suggesting that the Src pathway is important for *SPHK1* transcription. On the basis of these results, we focused on the mechanism of increased *SPHK1* mRNA by *v-Src*.

siRNA of SPHK1 inhibited cell proliferation of v-Src-*transformed NIH3T3*

v-Src-NIH3T3 showed higher cell proliferation on day 4 (Figure 2a) as well as anchorage-independent growth (data not shown) compared to mock-NIH3T3. Enhanced cell proliferation of *v-Src*-NIH3T3 was significantly inhibited by siRNA of *SPHK1* but not by scramble siRNA (Figure 2b). However, these effects

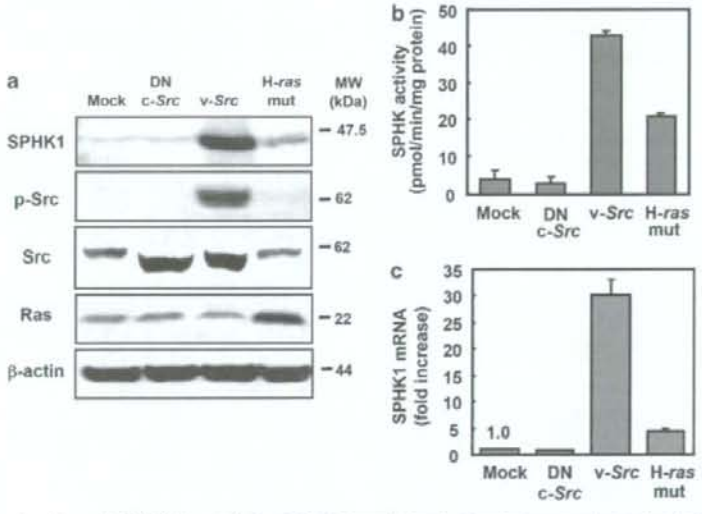

Figure 1 (**a**) Sphingosine kinase 1 (SPHK1) protein level. Stable transfectants of control expression vector (pcDNA3.1), dominant-negative (DN) *c-Src*, *v-Src* and mutated *H-Ras* expression vectors were analysed for SPHK1 expression. Expression of Src or Ras was also confirmed using anti-Src and anti-Ras antibody, respectively. β-Actin was used as the internal control. Anti-p-Src antibody detects phosphorylated (activated) Src protein. (**b**) SPHK enzyme activity of each transfectant described in Figure 1a was measured in triplicate as described in 'Materials and methods'. (**c**) *SPHK1* mRNA level. *SPHK1* mRNA was measured by quantitative reverse transcriptase (RT)–PCR method as described in 'Materials and methods'. mRNA level was expressed as SPHK1/β-actin, and the relative ratio of mock-NIH3T3 was regarded as 1.0. Assay was done in triplicate and results described were the mean from three different experiments.

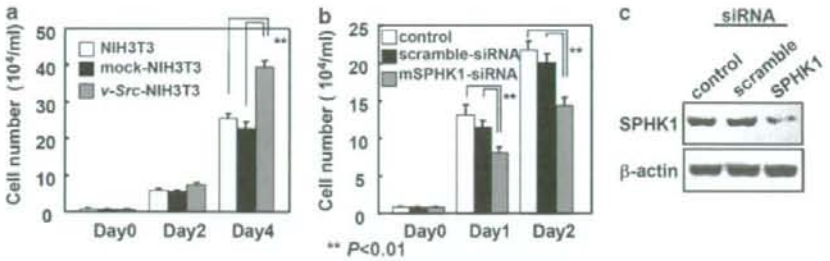

Figure 2 Cell proliferation of *v-Src*-NIH3T3 and the effect of siRNA of sphingosine kinase 1 (*SPHK1*). (**a**) Cell growth of original NIH3T3 cells, control vector (mock)-NIH3T3 cells and *v-Src*-NIH3T3 cells is shown. Initial plating cell density was 1×10^4 per ml. The cell growth of mock-NIH3T3 cells was not different from that of NIH3T3 cells. Statistical significance was determined on day 4 by Student's *t*-test. ** denotes $P<0.01$. (**b**) Effect of siRNA of *SPHK1* (si*SPHK1*). siRNA of *SPHK1* or scramble siRNA was transfected into *v-Src*-NIH3T3 as described in 'Materials and methods'. After 24 and 48 h, the cell number was analysed. ** denotes $P<0.01$. (**c**) Effect of each siRNA on SPHK1 protein expression is shown. β-Actin was used as the internal control.

were less remarkable in mock-NIH3T3 (data not shown). Inhibition of SPHK1 protein expression by siRNA for *SPHK1* is shown in Figure 2c.

Effect of inhibitors of signal transduction on SPHK1 protein expression

Previous reports have shown that many signaling proteins are involved in *v-Src*-induced NIH3T3 transformation, including ERK, c-Jun NH_2-terminal kinase 1 (JNK1) and signal transducers and activators of transcription 3 (Stat3; Greulich *et al*., 1996; Stofega *et al*., 1997; Turkson *et al*., 1999). Our *v-Src*-NIH3T3 also showed the activation of protein kinase C-α (PKCα), Stat3 and JNK, but not PKCδ, ERK, p38 mitogen-activated protein kinase or AKT activation (Figure 3a and data not shown). The effect of various inhibitors of these signaling components on the SPHK1 protein expression of *v-Src*-NIH3T3 was examined (Figure 3b). A pan-PKC (p-PKC) inhibitor, calphostin C, and a PKCα inhibitor, Go6976, inhibited SPHK1 protein expression in *v-Src*-NIH3T3. A JNK1 inhibitor (SP600125) and a cell-permeable Stat3 inhibitor also inhibited the SPHK1 protein level.

Promoter analysis and nuclear run-on assay

On the basis of our previous reports, increased *SPHK1* mRNA is considered to be due to its enhanced transcription (Nakade *et al*., 2003; Sobue *et al*., 2005). Figure 3c shows the promoter analysis of mouse *SPHK1a* gene. The promoter region covering −791 to −4 bp of 5′ of *SPHK1a* showed no significant change in the promoter activity between *v-Src*-NIH3T3 and mock-NIH3T3. Figure 3d shows the nuclear run-on analysis of mock-NIH3T3 and *v-Src*-NIH3T3. A newly synthesized *SPHK1* mRNA was also not significantly changed, which supports the promoter analysis. On the contrary, the treatment of NIH3T3 cells with a phorbol ester, phorbol 13-myristate 12-acetate (PMA), increased *SPHK1* mRNA about 2.5-fold.

v-Src *elongated* SPHK1 *mRNA half-life*

Unexpectedly, our analysis suggested the possibility that *v-Src* increased *SPHK1* mRNA by mRNA stabilization. Figure 4a illustrates the mRNA half-life of *SPHK1*, indicating that in NIH3T3 it was very short, about 10–15 min, whereas it was remarkably elongated, approximately 100 min, in *v-Src*-NIH3T3. Go6976 and calphostin C (Figure 4b) significantly decreased *SPHK1* mRNA half-life of *v-Src*-NIH3T3, suggesting the positive role of PKCα on *SPHK1* mRNA stabilization in *v-Src*-NIH3T3. We examined *SPHK1* mRNA by transiently transfecting *PKCα*, *Stat3* and *JNK1*-expression vector into NIH3T3. Figure 4c shows that constitutively active PKCα, Stat3 and JNK1 increased *SPHK1* mRNA, though the increased mRNA by *Stat3* and *JNK1* transfection was much less. On the basis of these results, we conclude that at least the PKC signaling pathway plays a role in the mRNA stabilization.

Effect of 3′-untranslated region of SPHK1 *on its mRNA half-life*

It is known that the AU-rich element (ARE) in the 3′ UTR is involved in mRNA decay (Meyer *et al*., 2004). The luciferase assay has been used for examining the involvement of 3′ UTR in mRNA half-life. Figure 4d illustrates the effect of 3′ UTR on luciferase activity as the index of *SPHK1* mRNA stability. The addition of full-length 3′ UTR inhibited luciferase expression in mock-NIH3T3. However, the luciferase activity was relatively well maintained in *v-Src*-NIH3T3, suggesting that *v-Src* inhibited *SPHK1* mRNA decay through this 3′ UTR. Because 3′ UTR of *SPHK1* does not contain the consensus AUR, which is the hallmark of a mRNA decay signal, we divided this 3′ UTR into two parts. The decrease in luciferase activity of the second but not the first half of 3′-UTR-luciferase vector was observed in mock-NIH3T3 (Figure 4d). The examination of the 5′ UTR of *SPHK1* showed no positive results (data not shown).

Two AUBPs, AUF1 and HuR, in v-Src-*NIH3T3*

We next examined two AUBPs, AUF1 and HuR (Kloss *et al*., 2004; Lal *et al*., 2004; Raineri *et al*., 2004). AUF1 is responsible for mRNA decay by binding to ARE and transferring the complex to the degradation

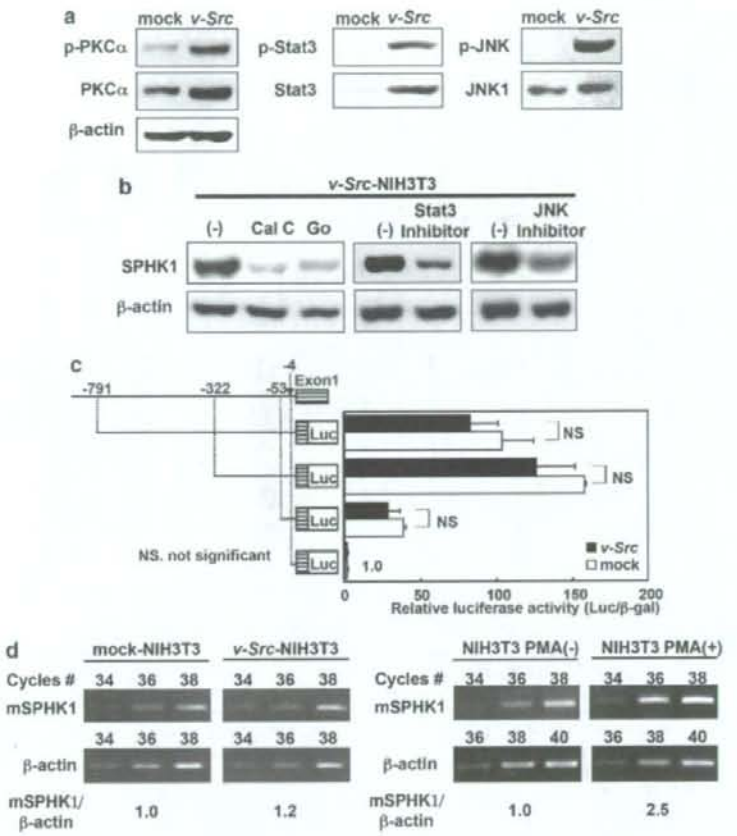

Figure 3 (**a**) Western blotting of various signaling components of mock-NIH3T3 and *v-Src*-NIH3T3. Anti-p-PKCα (pan-protein kinase C-α), anti-PKCα, anti-p-Stat3 (signal transducers and activators of transcription 3), anti-Stat3, anti-p-JNK1 (c-Jun NH_2-terminal kinase 1), anti-JNK1 and anti-β-actin antibodies were used to detect respective protein expressions in mock-NIH3T3 and *v-Src*-NIH3T3. β-Actin was used as the internal control. (**b**) Effect of signal transduction inhibitors on sphingosine kinase 1 (SPHK1) expression in *v-Src*-NIH3T3 cells. Inhibitors used were calphostin C (CalC, p-PKC inhibitor, 200 nM), Go6976 (Go, PKCα inhibitor, 1 μM), Stat3 inhibitor (100 μM) and cell-permeable JNK inhibitor I (50 μM). β-Actin was used as the internal control. (**c**) 5′-Promoter analysis. Promoter of *SPHK1* was analysed using mock-NIH3T3 and *v-Src*-NIH3T3 cells. Left side shows the construct of each promoter region whereas the right side shows the relative promoter activity expressed as respective luciferase activity/β-gal. Experiments were performed in triplicate and were repeated at least three times. NS, not significant. (**d**) Nuclear run-on assay of SPHK1 of mock-NIH3T3 and *v-Src*-NIH3T3 cells was performed as described in 'Materials and methods'. *SPHK1* mRNA level was evaluated as the ratio of SPHK1/β-actin. PCR cycles are shown as cycle no. Data of phorbol 13-myristate 12-acetate (PMA, 10^{-7} M)-treated mock-NIH3T3 cells are shown as a positive example of this assay method. Experiments were repeated at least twice with similar results.

system (Chen *et al*., 2001). Most ELAV (embryonic lethal abnormal vision)/Hu proteins (HuA, HuB, HuC and HuD) are present in neuronal tissue, whereas HuR protein is ubiquitously expressed and stabilizes mRNA decay by binding to ARE (Good, 1992).

Interestingly, a considerable decrease of AUF1 but not HuR protein was observed in *v-Src*-NIH3T3 as compared to mock-NIH3T3 (Figure 5a). In addition, increased tyrosine-phosphorylated AUF1 was observed in *v-Src*-NIH3T3. Furthermore, an increase in serine-phosphorylated HuR was observed in *v-Src*-NIH3T3 either by immunoprecipitation with anti-HuR antibody followed by western blotting with an antiphosphoserine PKC substrate antibody, or by immunoprecipitation with an antiserine/threonine antibody followed by western blotting with an anti-HuR antibody (Figure 5b). siRNA of *AUF1* greatly increased the *SPHK1* mRNA of mock-NIH3T3, whereas siRNA of *HuR* inhibited the *SPHK1* mRNA of *v-Src*-NIH3T3 (Figure 5c). Overexpression of AUF1 decreased *SPHK1* mRNA of *v-Src*-NIH3T3 (Figure 5d, left). Transfection of constitutively active PKCα induced serine-phosphorylated HuR of mock-NIH3T3 and increased its *SPHK1* mRNA level (Figure 5d, right; Figure 4c).

RNA immunoprecipitation

In order to confirm that the binding of 3′ UTR of *SPHK1* and AUF1 as well as HuR proteins was

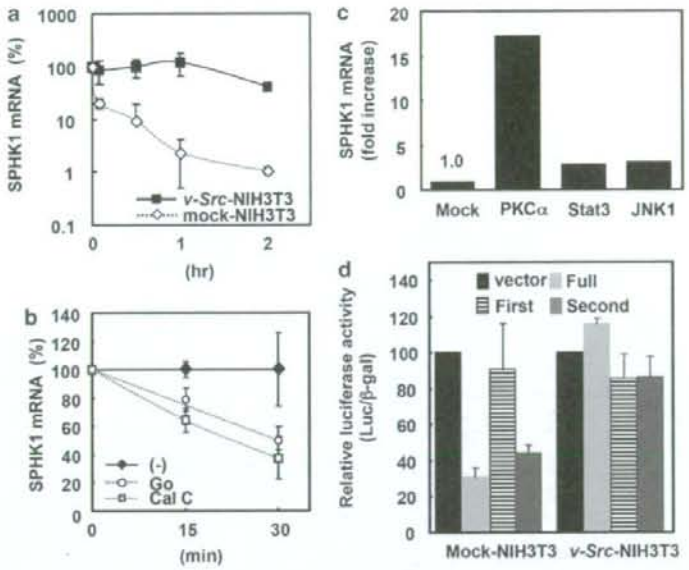

Figure 4 Half-life of sphingosine kinase 1 (*SPHK1*) mRNA. (**a**) Half-life of *SPHK1* mRNA was analysed using mock-NIH3T3 and *v-Src*-NIH3T3 as described in 'Materials and methods'. Actinomycin D was used at a concentration of 5 μg/ml. The *SPHK1* mRNA level before actinomycin D addition was regarded as 100%. (**b**) The effect of Go6976 and calphostin C on SPHK1 mRNA half-life of *v-Src*-NIH3T3. *v-Src*-NIH3T3 was treated with or without calphostin C (200 nM) and Go6976 (1 μM). *SPHK1* mRNA was measured by quantitative reverse transcriptase (RT)–PCR. (**c**) Effects on *SPHK1* mRNA of overexpressing constitutively active protein kinase C-α (PKCα), signal transducers and activators of transcription 3 (Stat3) and c-Jun NH_2-terminal kinase 1 (JNK1). Constitutively active PKCα, JNK1, Stat3 expression vector as well as pcDNA3.1 were transfected into NIH3T3 cells by the calcium precipitation method. Two days after transfection, *SPHK1* mRNA levels were measured. The level with a mock empty vector (pcDNA3.1) was regarded as 1.0. Experiments were repeated at least three times with similar results. (**d**) Effects of 3′ UTR on mRNA stability were examined using luciferase vectors with or without 3′-UTR insertion as described in 'Materials and methods'. Each luciferase vector was transfected into mock-NIH3T3 and *v-Src*-NIH3T3. After 24 h, luciferase activity was examined and was corrected with β-gal activity. Experiments were performed in triplicate and were repeated at least three times. Mean ± s.d. is shown. Relative luciferase activity of vectors without 3′ UTR was regarded as 100%. Vector: vector without 3′-UTR insert, full: full-length 3′-UTR insert; first: the first half of 3′-UTR insert; second: the second half of 3′-UTR insert.

involved in the mRNA decay, we performed an RNA-chromatin immunoprecipitation assay (RNA-ChIP) described by Pan *et al.* (2005). Both mock-NIH3T3 and *v-Src*-NIH3T3 were subjected to RNA immunoprecipitation as described in 'Materials and methods'. Figure 6a shows that AUF1 but not HuR was bound to 3′ UTR of *SPHK1* in mock-NIH3T3, whereas HuR but not AUF1 was bound to 3′ UTR of *SPHK1* in *v-Src*-NIH3T3. The binding of HuR to the 3′ UTR of *SPHK1* was inhibited by the p-PKC inhibitor, calphostin C, and the PKCα inhibitor, Go6976, but not the PKCδ inhibitor, rottlerin (Figure 6b). This suggests that the difference in the decay rate of SPHK1 observed in these two cells was mainly due to the binding of a different AUBP (or the relative ratio of these AUBPs) to the 3′ UTR of *SPHK1* mRNA. In order to confirm the binding of AUBPs and 3′ UTR of *SPHK1* further, we examined the binding of 3′ UTR and AUBPs by a biotin-labeled RNA-pull-down assay. After collecting complexes of the biotinylated RNA and binding proteins by streptavidin-conjugated beads, binding proteins were identified by western blotting. Using the full-length 3′ UTR, HuR binding was identified in *v-Src*-NIH3T3 but not in mock-NIH3T3 (Figure 6c, left). Probably because of the limited abundance of AUF1, we could not obtain the positive signal for AUF1 (data not shown). Among the eight biotin-labeled RNA fragments of 3′ UTR of *SPHK1*, positive signals were observed in the fragments 7 and 8 located at the most 3′ end of 3′ UTR (Figures 6c, right). Interestingly, a difference of band intensity between mock- and vSrc-NIH3T3 was observed in fragment 8, suggesting that more HuR was bound to this region in *v-Src*-NIH3T3, whereas in mock-NIH3T3, AUF1 binding to the same region was predominant.

Discussion

Recently, Xia *et al.* (2000) reported that mutated *H-Ras* increases SPHK enzyme activity. In our study, *v-Src* was found to increase SPHK enzyme activity, *SPHK1* mRNA and SPHK1 protein expression in either transient or stable transfectants. We also established a stable DN-*c-Src*-NIH3T3 without an increase in SPHK enzyme activity, suggesting that enhanced *SPHK1* expression is due to the intrinsic *v-Src* functions.

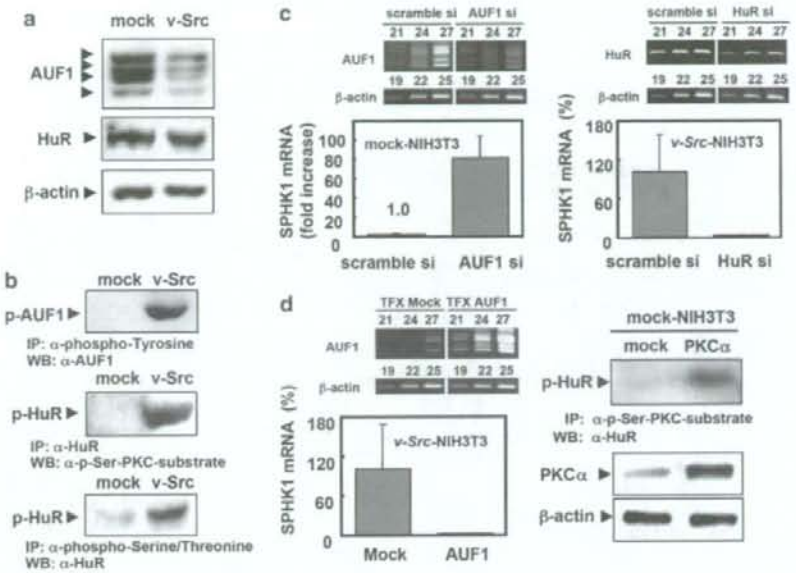

Figure 5 Two AUBPs (AU-rich region-binding proteins: AUF1 and HuR) and sphingosine kinase 1 (*SPHK1*) mRNA. (**a**) AUF1 and HuR protein levels. In the upper part, AUF1 and HuR proteins of mock-NIH3T3 and *v-Src*-NIH3T3 are illustrated. It is worth noting that AUF1 was composed of four isoforms, p45, p40/42 and p37. (**b**) Upper: tyrosine-phosphorylated (p)-AUF1 protein levels. Tyrosine-phosphorylated AUF1 was examined by immunoprecipitation with an antiphosphotyrosine antibody followed by an anti-AUF1. It is of note that no significant change in serine/threonine-phosphorylated AUF1 was observed between mock-NIH3T3 and v-Src-NIH3T3 (data not shown). Middle and lower: phosphorylated (p)-HuR protein levels. An antiserine-phosphorylated protein kinase C (PKC) substrate antibody was used after immunoprecipitating with an anti-HuR antibody (upper part). Similarly, phosphorylated-HuR was examined by immunoprecipitation with an antiserine/threonine-phosphorylated antibody followed by western blotting with an anti-HuR antibody (lower part). (**c**) Effects of siRNA for *AUF1* and *HuR*. siRNA of *AUF1* and siRNA of *HuR* were transfected into mock-NIH3T3 and *v-Src*-NIH3T3, respectively. Upper part shows the inhibition of mRNA level by siRNA. Experiments were performed in triplicate, and the results were expressed as mean ± s.d. *SPHK1* mRNA observed in scramble siRNA-treated cells was regarded as the control, respectively. (**d**) Left: *AUF1* expression vector was introduced transiently into *v-Src*-NIH3T3. Two days after transfection, *SPHK1* mRNA was evaluated by quantitative reverse transcriptase (RT)–PCR. Upper part shows *AUF1* mRNA level. Mean ± s.d. was calculated from three separate experiments. The data of mock vector (pcDNA3.1)-treated cells were determined as 100%. Right: phospho-HuR protein level of constitutive active PKCα-transfected mock-NIH3T3; constitutively active PKCα was transiently transfected into mock-NIH3T3. Two days after the transfection, phospho-HuR was detected by immunoprecipitation with an antiphosphoserine-PKC substrate antibody followed by western blotting with an anti-HuR antibody. Increased PKCα protein level in PKCα-transfected mock-NIH3T3 cells is illustrated in the lower part.

Western blotting with an antiphosphorylated Src antibody confirmed the activated status of Src in *v-Src*-NIH3T3 (Figure 1a).

The enhanced expression of SPHK1 by *v-Src* (Figure 1c) does not take place at the level of translation as reported in the case of a hypoxia-inducible factor (HIF)-1 (Karni *et al.*, 2002), but at the post-transcriptional level. The involvement of SPHK1 in the enhanced proliferation of *v-Src*-NIH3T3 compared to mock-NIH3T3 was demonstrated using siRNA for *SPHK1* (Figure 2b). The partial inhibition of cell growth of *v-Src*-NIH3T3 by siRNA for *SPHK1* suggests that SPHK1 is not the sole factor in *v-Src*-induced transformation.

Analysis of the signal-transduction pathway of *v-Src*-NIH3T3 revealed that PKCα, JNK1 and Stat3, but not Stat5 (data not shown), were highly activated in *v-Src*-NIH3T3. These results were consistent with those of previous reports (Greulich *et al.*, 1996; Stofega *et al.*, 1997; Turkson *et al.*, 1999). Various inhibitors of PKCα, Stat3 and JNK revealed their positive involvement in SPHK1 expression (Figure 3b). However, the interrelationship between these factors remains to be determined.

Stable and transient *v-Src* expression induces a number of gene products (Tezuka *et al.*, 1996). A *v-Src*-induced increase in target gene transcription was reportedly mediated by various cellular signaling pathways or transcription factors such as MEKK1/JNK and raf/MEK/ERK pathways (Xie and Herschman, 1995) or Sp1 and EGR-1 (Qureshi *et al.*, 1991; Kuo *et al.*, 2006). In these studies, promoter analysis clearly showed that *v-Src* increased target gene transcription. However, our present analysis showed that the promoter activity revealed no significant difference between *v-Src*-NIH3T3 and mock-NIH3T3 (Figure 3c). Moreover, the nuclear run-on assay (Figure 3d) failed to show any significant increase in the transcription rate of *SPHK1* in *v-Src*-NIH3T3 compared to mock-NIH3T3, whereas PMA increased *de novo* transcription about 2.5-fold. We have reported that the 5′-promoter region is mainly

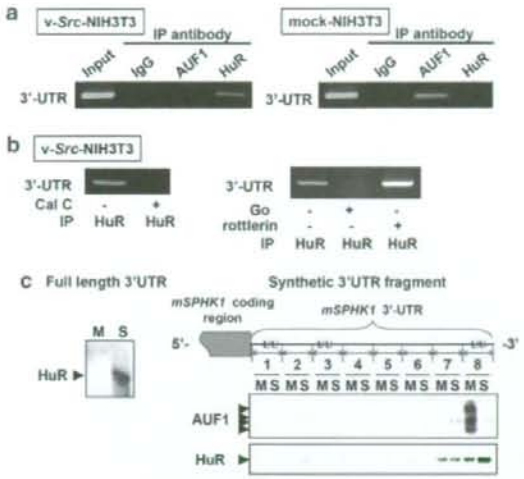

Figure 6 RNA chromatin immunoprecipitation assay. (**a**) Mock-NIH3T3 and *v-Src*-NIH3T3 were fixed with 1% formaldehyde and immunoprecipitated with an anti-AUF1, anti-HuR or control antibody. After extracting RNA from respective samples, reverse transcriptase (RT)–PCR was performed according to 'Materials and methods'. (**b**) The effect of calphostin C (200 nM), Go6976 (1 μM) and rottlerin (2.5 μM) was examined in this assay using *v-Src*-NIH3T3 cells. (**c**) Biotinylated RNA-pull-down assay. Left: biotin-labeled full-length 3′ UTR of sphingosine kinase 1 (SPHK1) mRNA (15 μg), prepared by *in vitro* transcription described in the Supplementary information, was incubated with 100 μg of mock- (M) or *v-Src*-NIH3T3 (S) cytoplasmic extract, and the complexes were collected by Dynabeads as described in the 'Materials and methods'. Protein components of the complexes were identified by western blotting using an anti-HuR antibody. In case of AUF1, the incubation of more cytoplasmic extract did not show any significant signal, probably due to the limited amount of AUF1 protein (data not shown). Right: eight biotin-labeled synthetic fragments of 3′ UTR of SPHK1 mRNA (2 μg each) were incubated with the cytoplasmic extract (100 μg for AUF1 and 15 μg for HuR) of mock- (M) and *v-Src*-NIH3T3 (S), and the complexes were collected by Dynabeads as described in the 'Materials and methods'. Protein components of the complexes were identified by western blotting using either an anti-AUF1 or an anti-HuR antibody. The upper part illustrates each fragment, whose sequence is available in Supplementary information. Although the consensus AU-rich sequence was not present, a stretch of UUU was illustrated as **UU** as the candidate *cis*-element for the AU-rich region-binding protein (AUBP) binding.

involved in *SPHK1* transcription when activated by agonists including PMA, cytokines, NGF and glial cell line-derived neurotrophic factor (Nakade *et al.*, 2003; Sobue *et al.*, 2005; Murakami *et al.*, 2007). Thus, these results suggest that an increase of *v-Src*- and PMA-induced *SPHK1* mRNA was mediated by different mechanisms.

SPHK1 mRNA abundance is determined by the rates of transcription and mRNA decay. The elongation of *SPHK1* mRNA half-life was observed in *v-Src*-NIH3T3 (Figure 5). In cells transformed by v-Src, PKCα, Stat3 and JNK1 were overexpressed and activated (Borner *et al.*, 1992). The relationship between PKC and Stat3 was previously reported (Park *et al.*, 2002, Gartsbein *et al.*, 2006), suggesting that Stat3 is located downstream of PKC. The JNK pathway was involved in *IL-2* mRNA stabilization (Chen *et al.*, 1998). Although transient transfection of these genes was shown to increase *SPHK1* mRNA (Figure 4c), further analysis is needed to elucidate how these components act in signaling by *v-Src* in the *SPHK1* mRNA decay. Because PKCα expression induced the highest SPHK1 mRNA (Figure 4c), we further examined the involvement of PKCα. The involvement of PKC in mRNA half-life elongation (Hanford and Glembotski, 1996; Shih *et al.*, 1999) was reported previously.

A model of regulated mRNA decay has been proposed (Meyer *et al.*, 2004). Two types of proteins have been reported to be involved in this process; one is the mRNA decay-accelerating factors (AUF1 and TTP) and the other is an mRNA decay-inhibiting factor (HuR; Wilusz *et al.*, 2001), both of which bind to 3′ UTR of mRNA. In our case, 3′ UTR of *SPHK1* has no AUUA or UUAUUUA sequence. However, the absence of typical ARE does not necessarily exclude the mRNA decay through 3′ UTR. Very few among the stabilized genes in malignant T cells have the consensus AREs (Vlasova *et al.*, 2005) although AUBP was not precisely analysed. Our reporter assay using a luciferase vector containing the 3′ UTR of *SPHK1* (Figure 4d) was consistent with the elongation of mRNA half-life and also revealed that a decrease in luciferase activity due to 3′ UTR was much less in *v-Src*-NIH3T3 than in mock-NIH3T3. Our results suggest that the inhibition of *SPHK1* mRNA decay by a *v-Src*-mediated signaling pathway is involved in the growth advantage of *v-Src*-NIH3T3, and that the second part of 3′ UTR is important in the mRNA decay.

Recently, Bromann *et al.* (2005) reported that platelet-derived growth factor stimulates the *c-Src*-dependent mRNA stabilization of specific early genes. In *v-Src*-transformed chick embryofibroblasts, E3/pCEF4 mRNA was stabilized with its 3′ UTR containing the AUUUA sequence (Stoeckle and Hanafusa, 1989; Blobel and Hanafusa, 1991). Fawal *et al.* (2006) reported that nucleophosmin-anaplastic lymphoma kinase phosphorylates AUF1 and elongates the half-life of ARE-containing mRNAs. NPM/ALK was also reported to activate *c-Src* so as to mediate its mitogenicity (Cussac *et al.*, 2004). Therefore, it is likely that *v-Src* phosophorylates tyrosine residues of AUF1 and inhibits its mRNA decay activity.

In the current study, AUF1 protein expression in *v-Src*-NIH3T3 was greatly diminished whereas the tyrosine-phosphorylated form was increased and *v-Src*-phosphorylated HuR was increased in *v-Src*-NIH3T3 compared to mock-NIH3T3, although the total HuR protein levels were identical between the two (Figure 5a). The decrease in total AUF1 protein and increased tyrosine-phosphorylated form of AUF1 as well as phosphorylated HuR might be effective in *SPHK1* mRNA stabilization. HuR phosphorylation could also be detected by antiserine-phosphorylated PKC substrate antibody, suggesting PKC induced HuR phosphorylation in *v-Src*-NIH3T3. Lopez de Silanes *et al.* (2004) examined target genes (motifs) of HuR

protein and identified *SPHK1* mRNA as a target of HuR (Supplementary data of Lopez de Silanes *et al.*, 2004). Furthermore, Doller *et al.* (2007) recently reported PKCα phosphorylates HuR leading to the stabilization of *cyclooxygenase-2* mRNA.

We have shown the signaling pathway extending from v-Src to PKCα activation and HuR phosphorylation, thereby leading to the binding of activated HuR to 3′ UTR of *SPHK1*. Because PKC is a serine/threonine kinase, the upstream signaling of tyrosine phosphorylation of AUF1 might not be through PKC (Wilson *et al.*, 2003), and further experiments are needed. The involvement of AUF1 and HuR in *SPHK1* mRNA half-life in *v-Src*-NIH3T3 was further supported by siRNA transfection and overexpression experiments (Figures 5c and d), indicating the unique and significant role of AUF1 and HuR. Furthermore, direct binding of AUF1 to 3′ UTR of *SPHK1* was detected in the RNA-ChIP assay and RNA-pull-down assay (Figures 6a–c and 7), suggesting that AUF1 is involved in *SPHK1* mRNA decay in mock-NIH3T3, and that HuR is implicated in *SPHK1* mRNA stabilization in *v-Src*-NIH3T3 at least through the most 3′ part of 3′ UTR. A UUUU sequence in this fragment might be the candidate of *cis*-element in binding, however, further analysis is needed.

Taken together, the current study demonstrated, for the first time, that the *SPHK1* mRNA half-life is relatively short in noncancerous cells and that its stabilization by PKC and probably other signaling pathways is involved in its increased expression. Effective growth inhibition by siRNA of SPHK1 of *v-Src*-NIH3T3, in which overexpression of SPHK1 was due to the accumulation of its mRNA, suggests the possible application of SPHK inhibitors or siRNA as a strategy of novel cancer treatment.

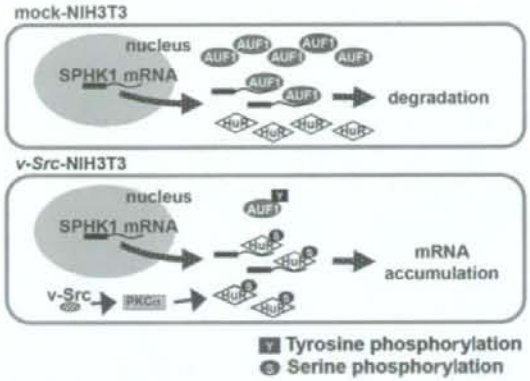

Figure 7 Schematic presentation of AU-rich region-binding proteins (AUBPs) binding to 3′ UTR of sphingosine kinase 1 (*SPHK1*). In mock-NIH3T3, *SPHK1* mRNA degradation occurred, as the AUF1 level was higher than that of *v-Src*-NIH3T3. In contrast, decrease in AUF1, tyrosine phosphorylation of AUF1 and increase in serine-phosphorylated HuR may promote the stabilization of the *SPHK1* mRNA in *v-Src*-NIH3T3.

Materials and methods

Cell lines and reagents

Stable *v-Src* transformants of NIH3T3 cells were prepared by transfecting pcDNA3.1- (Invitrogen, Carlsbad, CA, USA) containing *v-Src*, which was a gift from Dr M Hamaguchi (Nagoya University School of Medicine). DN *c-Src* expression vector was from Dr CSS Wong (Hong Kong University, Hong Kong, China). *H-Ras* (V12G)-NIH3T3 was derived from Dr K Furukawa (Nagoya University School of Medicine). Mock-NIH3T3 cells were prepared by transfecting pcDNA3.1 to NIH3T3. Constitutive active *Stat3* expression vector was from Dr A Iwama (Chiba University, Chiba, Japan). *JNK1* expression vector was the gift of Dr A Atfi (INSERM U482, Hospital Saint-Antoine, Paris, France). Constitutive active *PKCα* expression vector was from Dr Jae-Won Soh (Inha University, Inchon, Korea).

AUF1 expression vector was from Dr Y Arao (National Institute of Environmental Health Sciences, USA). *HuR* expression vector was the generous gift of Dr J Hauber (Heinrich-Pette Institut, Hamburg, Germany). siRNAs for *AUF1*, *HuR* and mouse *SPHK1* were purchased from Sigma Genosys (Hokkaido, Japan). Their sequences were described in the Supplementary information.

Go6976, calphostin C, rottlerin, cell-permeable Stat3 inhibitor and JNK1 inhibitor (SP600125) were from Calbiochem (La Jolla, CA, USA).

Viable cell counting

Viable cells were measured in triplicate by trypan blue dye exclusion. The effect of siRNA of *SPHK1* on cell proliferation was examined 2 days after transfecting either siRNA of *SPHK1* or scramble siRNA to NIH3T3.

SPHK enzyme activity

SPHK enzyme activity was measured as described previously (Sobue *et al.*, 2005). Our assay mainly detected SPHK1 but not SPHK2 enzyme activity because of the presence of 0.25% Triton X-100 and the absence of 1 M KCl in the reaction mixture (Liu *et al.*, 2000).

Western blotting

Western blotting using antimouse SPHK1 antibody was performed as described previously (Sobue *et al.*, 2005). Other antibodies used were as follows: anti-Src antibody and anti-AUF1 antibody (Upstate Biotechnology, Lake Placid, NY, USA), anti-phospho-Src family (Tyr416) antibody (Cell Signaling Technology, Danvers, MA, USA), anti-β-actin antibody (Cytoskeleton Inc., Denver, CO, USA), anti-ERK, anti-p-ERK, anti-AKT, anti-p-AKT, anti-p38, anti-p-p38, anti-Stat3, anti-p-Stat3, anti-JNK1, anti-p-JNK1, anti-PKCα, anti-p-PKCs and anti-HuR antibody (Santa Cruz Biotechnology Inc., Santa Cruz, CA, USA), antiphosphotyrosine antibody (Calbiochem, San Diego, CA, USA), antiphosphoserine/threonine antibody (Upstate Biotechnology) and antiserine-phosphorylated PKC substrate antibody (Cell Signaling Technology, Beverly, MA, USA).

Quantitative and semiquantitative RT–PCR

Real-time quantitative RT–PCR was performed according to the method described previously (Sobue *et al.*, 2006) with minor modifications. *SPHK1* mRNA was calculated as the ratio of *SPHK1* mRNA to *β-actin* mRNA. For the nuclear run-on assay of *mSPHK1*, semiquantitative RT–PCR method was used according to Sobue *et al.* (2005). Further information was provided as Supplementary information.

Promoter activity

Mouse *SPHK1a* promoter was cloned by the PCR method. The method was provided as Supplementary information. pGL3 basic vectors containing 791, 322, 53 and 4 bp of the 5′ promoter of *mSPHK1a* were used as shown in Figure 3c. Reporter construct (5 μg) and β-gal expression vector (1 μg) were co-transfected to either mock-NIH3T3 or *v-Src*-NIH3T3 by the calcium precipitation method. Relative promoter activity was expressed as luciferase activity/β-gal. The value of luc-4/pGL3 in mock- and *v-Src*-NIH3T3 was determined as 1.0, respectively.

Nuclear run-on assay

The rate of mature *SPHK1* transcription was determined by the nuclear run-on assay as described previously (Patrone *et al*., 2000). Harvested cells were resuspended in 4 ml of Nonidet P-40 (NP-40) lysis buffer containing 10 mM Tris-HCl (pH 7.4), 10 mM NaCl, 3 mM $MgCl_2$ and 0.5% NP-40 for 5 min at 4 °C. After collecting nuclei, they were resuspended in 100 μl of glycerol buffer containing 50 mM Tris-HCl (pH 8.3), 40% glycerol, 5 mM $MgCl_2$ and 0.1 mM EDTA. They were stored at −30 °C until use. Nuclear run-on and RNA isolation were performed in the presence of biotin-16-UTP (Roche, Mannheim, Germany). Dynabeads M-280 (Dynal Biotech, Oslo, Norway), which were used to capture the biotin-labeled molecules from the purified nuclear RNA, were washed once with 15% formamide and twice with 2 × SSC and resuspended in 8.5 μl of diethylpyrocarbonate-treated H_2O before preparing cDNA using random hexamer. Semiquantitative RT–PCR was then performed as described in the previous RT–PCR section.

mRNA half-life

The half-life of mRNA was measured according to Fritz *et al*. (1995) and Leclerc *et al*. (2002). Briefly, logarithmically growing cells were treated with 5 μg/ml actinomycin D. After an indicated incubation period (15–120 min), total RNA was isolated for quantitative RT–PCR as described in the previous section. The relative mRNA level of *SPHK1* (*SPHK1*/*β-actin*) before actinomycin D treatment was defined as 100%, and the half-life of *SPHK1* mRNA was calculated.

Effects of 3′- and 5′-untranslated region (3′ UTR and 5′ UTR) of mouse *SPHK1* on its mRNA half-life. To analyse the involvement of 3′ UTR of mouse *SPHK1* in its mRNA decay, 3′ UTR of mouse *SPHK1* was cloned. Description of cloning was provided as Supplementary information. pGL3 promoter vectors containing 283 bp (full length) 3′ UTR, 138 bp (the first half) 3′ UTR and 145 bp (the second half) 3′ UTR were used for experiments. A total of 0.5 μg of this vector and 0.2 μg of the β-gal expression vector were transfected into *v-Src*- or mock-NIH3T3 cells. Similarly, 5′ UTR of *mSPHK1a* was also cloned as described in Supplementary information. The corrected luciferase activity (Luc/β-gal) was calculated as the parameter of *SPHK1* mRNA decay.

Modulation of AUF1 and HuR gene expression

Overexpression of AUF1 in *v-Src*-NIH3T3 was performed using FuGENE6 (Roche). siRNAs of *AUF1*, *HuR* as well as scramble siRNA were transfected using FuGENE6 according to the recommendation of the manufacturer.

RNA-chromatin immunoprecipitation assay

An RNA-ChIP assay was performed according to Pan *et al*. (2005). Briefly, cultured cells were treated with 1% formaldehyde at 37 °C for 15 min, and lysed with nuclei-swelling buffer. After sonication and centrifugation, cytoplasmic extract was incubated at 4 °C overnight with 5 μg of either anti-AUF1, anti-HuR or nonspecific control antibody. Cytoplasmic extract not incubated with antibody was saved as an input sample. The antibody-bound complex was precipitated by protein A-Sepharose beads (Amersham Biosciences, Little Chalfont, Buckinghamshire, UK). The beads were washed and the protein–RNA complex was eluted from the protein A-Sepharose beads with 250 μl of elution buffer (1% SDS and 0.1 M $NaHCO_3$) at 37 °C for 15 min. The RNA in the immunoprecipitated complex and the RNA in the previously saved input fraction were released by reversing the crosslinking at 65 °C for 2 h with 200 nM NaCl and 20 μg of proteinase K. RNA was then extracted from the solution and subjected to RT–PCR using primers to amplify a sequence in the 3′ UTR of *SPHK1* (upper 5′-CTCTGTGCCTTTGTCTACTCT-3′; lower 5′-TGGAAAAGTCTCTTTATTTGA-3′). The PCR conditions were 96 °C for 15 s, 54 °C for 30 s and 72 °C for 30 s, and 40 cycles.

Biotinylated RNA pull-down assay

In vitro transcription of the full-length 3′ UTR of *SPHK1* was described in the Supplementary information. We also prepared the eight 3′-UTR fragments (Thermo Fisher Scientific, Ulm, Germany) with a biotin attached to the 3′-terminus. Cytoplasmic proteins were extracted with Nuclear and Cytoplasmic Extraction Reagents (PIERCE, Rockford, IL, USA). Reaction mixture containing 1 × binding buffer (20 mM HEPES, pH 7.8, 50 mM KCl, 3 mM $MgCl_2$, 0.5 mM EDTA, 0.05% Triton X-100, 0.5 mM dithiothreitol), 80 μg tRNA, 1% bovine serum albumin, RNase inhibitor and biotinylated RNA (2–15 μg) were incubated at 4 °C for 30 min. Following the incubation, cytoplasmic proteins (15–100 μg) were added and incubated at 4 °C for 30 min. Ribonucleoprotein complexes were isolated using streptavidin-conjugated Dynabeads (Dynal Biotech). The presence of HuR/AUF1 in ribonucleoprotein complex was identified by western blot analysis with either an anti-HuR or anti-AUF1 antibody.

Statistical analysis

Results were expressed as mean ± s.d. Statistical analysis was performed using Student's *t*-test and analysis of variance for significance. *P*-values <0.01 were considered significant.

References

Akao Y, Banno Y, Nakagawa Y, Hasegawa N, Kim TJ, Murate T *et al*. (2006). High expression of sphingosine kinase 1 and S1P receptors in chemotherapy-resistant prostate cancer PC3 cells and their camptothecin-induced up-regulation. *Biochem Biophys Res Commun* **342**: 1284–1290.

Alvarez SE, Milstien S, Spiegel S. (2007). Autocrine and paracrine roles of sphingosine-1-phosphate. *Trends Endocrinol Metab* **18**: 300–307.

Bektas M, Jolly PS, Müller C, Eberle J, Spiegel S, Geilen CC. (2005). Sphingosine kinase activity counteracts ceramide-mediated cell death in human melanoma cells: role of Bcl-2 expression. *Oncogene* **24**: 178–187.

Blobel GA, Hanafusa H. (1991). The v-src inducible gene 9E3/pCEF4 is regulated by both its promoter upstream sequence and its 3′ untranslated region. *Proc Natl Acad Sci USA* **88**: 1162–1166.

Bonhoure E, Pchejetski D, Aouali N, Morjani H, Levade T, Kohama T *et al*. (2006). Overcoming MDR-associated chemoresistance in HL-60 acute myeloid leukemia cells by targeting sphingosine kinase-1. *Leukemia* **20**: 95–102.

Borner C, Guadagno SN, Hsiao WW, Fabbro D, Barr M, Weinstein IB. (1992). Expression of four protein kinase C isoforms in rat fibroblasts. Differential alterations in ras-, src-, and fos-transformed cells. *J Biol Chem* **267**: 12900–12910.

Bromann PA, Korkaya H, Webb CP, Miller J, Calvin TL, Courtneidge SA. (2005). Platelet-derived growth factor stimulates Src-dependent mRNA stabilization of specific early genes in fibroblasts. *J Biol Chem* **280**: 10253–10263.

Chen CY, Del Gatto-Konczak F, Wu Z, Karin M. (1998). Stabilization of interleukin-2 mRNA by the c-Jun NH2-terminal kinase pathway. *Science* **280**: 1945–1949.

Chen CY, Gherzi R, Ong SE, Chan EL, Raijmakers R, Pruijn GJ *et al.* (2001). AU binding proteins recruit the exosome to degrade ARE-containing mRNAs. *Cell* **107**: 451–464.

Cussac D, Greenland C, Roche S, Bai RY, Duyster J, Morris SW *et al.* (2004). Nucleophosmin-anaplastic lymphoma kinase of anaplastic large-cell lymphoma recruits, activates, and uses pp60c-src to mediate its mitogenicity. *Blood* **103**: 1464–1471.

Dehm S, Senger MA, Bonham K. (2001). SRC transcriptional activation in a subset of human colon cancer cell lines. *FEBS Lett* **487**: 367–371.

Dehm SM, Bonham K. (2004). SRC gene expression in human cancer: the role of transcriptional activation. *Biochem Cell Biol* **82**: 263–274.

Doller A, Huwiler A, Muller R, Radeke HH, Pfeilschifter J, Eberhardt W. (2007). Protein kinase C alpha-dependent phosphorylation of the mRNA-stabilizing factor HuR: implications for posttranscriptional regulation of cyclooxygenase-2. *Mol Biol Cell* **18**: 2137–2148.

Fawal M, Armstrong F, Ollier S, Dupont H, Touriol C, Monsarrat B *et al.* (2006). A 'liaison dangereuse' between AUF1/hnRNPD and the oncogenic tyrosine kinase NPM-ALK. *Blood* **108**: 2780–2788.

Frame MC. (2004). Newest findings on the oldest oncogene; how activated src does it. *J Cell Sci* **117**: 989–998.

French KJ, Schrecengost RS, Lee BD, Zhuang Y, Smith SN, Eberly JL *et al.* (2003). Discovery and evaluation of inhibitors of human sphingosine kinase. *Cancer Res* **63**: 5962–5969.

Fritz G, Kaina B, Aktories K. (1995). The ras-related small GTP-binding protein RhoB is immediate-early inducible by DNA damaging treatments. *J Biol Chem* **270**: 25172–25177.

Gartsbein M, Alt A, Hashimoto K, Nakajima K, Kuroki T, Tennenbaum T. (2006). The role of protein kinase C delta activation and STAT3 Ser727 phosphorylation in insulin-induced keratinocyte proliferation. *J Cell Sci* **119**: 470–481.

Good PJ. (1992). A conserved family of elav-like genes in vertebrates. *Proc Natl Acad Sci USA* **92**: 4557–4561.

Greulich H, Reichman C, Hanafusa H. (1996). Delay in serum stimulation of Erk activity caused by oncogenic transformation. *Oncogene* **12**: 1689–1695.

Hanford DS, Glembotski CC. (1996). Stabilization of the B-type natriuretic peptide mRNA in cardiac myocytes by alpha-adrenergic receptor activation: potential roles for protein kinase C and mitogen-activated protein kinase. *Mol Endocrinol* **10**: 1719–1727.

Karni R, Dor Y, Keshet E, Meyuhas O, Levitzki A. (2002). Activated pp60c-Src leads to elevated hypoxia-inducible factor (HIF)-1 alpha expression under normoxia. *J Biol Chem* **277**: 42919–42925.

Kawamori T, Osta W, Johnson KR, Pettus BJ, Bielawski J, Tanaka T *et al.* (2006). Sphingosine kinase 1 is up-regulated in colon carcinogenesis. *FASEB J* **20**: 386–388.

Kloss S, Srivastava R, Mulsch A. (2004). Down-regulation of soluble guanylyl cyclase expression by cyclic AMP is mediated by mRNA-stabilizing protein HuR. *Mol Pharmacol* **65**: 1440–1451.

Kuo L, Chang HC, Leu TH, Maa MC, Hung WC. (2006). Src oncogene activates MMP-2 expression via the ERK/Sp1 pathway. *J Cell Physiol* **207**: 729–734.

Lal A, Mazan-Mamczarz K, Kawai T, Yang X, Martindale JL, Gorospe M. (2004). Concurrent versus individual binding of HuR and AUF1 to common labile target mRNAs. *EMBO J* **23**: 3092–3102.

Leclerc GJ, Leclerc GM, Barredo JC. (2002). Real-time RT–PCR analysis of mRNA decay: half-life of beta-actin mRNA in human leukemia CCRF-CEM and Nalm-6 cell lines. *Cancer Cell Int* **2**: 1–5.

Liu H, Sugiura M, Nava VE, Edsall LC, Kono K, Poulton S *et al.* (2000). Molecular cloning and functional characterization of a novel mammalian sphingosine kinase type 2 isoform. *J Biol Chem* **275**: 19513–19520.

Lopez de Silanes I, Zhan M, Lal A, Yang X, Gorospe M. (2004). Identification of a target RNA motif for RNA-binding protein HuR. *Proc Natl Acad Sci USA* **101**: 2987–2992.

Meyer S, Temme C, Wahle E. (2004). Messenger RNA turnover in eukaryotes: pathways and enzymes. *Crit Rev Biochem Mol Biol* **39**: 197–216.

Murakami M, Ichihara M, Sobue S, Kikuchi R, Ito H, Kimura A *et al.* (2007). RET signaling-induced SPHK1 gene expression plays a role in both GDNF-induced differentiation and MEN2-type oncogenesis. *J Neurochem* **102**: 1585–1594.

Nakade Y, Banno Y, T-Koizumi K, Hagiwara K, Sobue S, Koda M *et al.* (2003). Regulation of sphingosine kinase 1 gene expression by protein kinase C in a human leukemia cell line, MEG-O1. *Biochim Biophys Acta* **1635**: 104–116.

Olivera A, Kohama T, Edsall L, Nava V, Cuvillier O, Poulton S *et al.* (1999). Sphingosine kinase expression increases intracellular sphingosine-1-phosphate and promotes cell growth and survival. *J Cell Biol* **14**: 545–558.

Pan YX, Chen H, Kilberg MS. (2005). Interaction of RNA-binding proteins HuR and AUF1 with the human ATF3 mRNA 3′-untranslated region regulates its amino acid limitation-induced stabilization. *J Biol Chem* **280**: 34609–34616.

Park YJ, Park ES, Kim MS, Kim TY, Lee HS, Lee S *et al.* (2002). Involvement of the protein kinase C pathway in thyrotropin-induced STAT3 activation in FRTL-5 thyroid cells. *Mol Cell Endocrinol* **194**: 77–84.

Patrone G, Puppo F, Cusano R, Scaranari M, Ceccherini I, Puliti A *et al.* (2000). Nuclear run-on assay using biotin labeling, magnetic bead capture and analysis by fluorescence-based RT–PCR. *Biotechniques* **29**: 1012–1014, 1016–1017.

Qureshi SA, Cao XM, Sukhatme VP, Foster DA. (1991). v-Src activates mitogen-responsive transcription factor Egr-1 via serum response elements. *J Biol Chem* **266**: 10802–10806.

Raineri I, Wegmueller D, Gross B, Certa U, Moroni C. (2004). Roles of AUF1 isoforms, HuR and BRF1 in ARE-dependent mRNA turnover studied by RNA interference. *Nucleic Acids Res* **32**: 1279–1288.

Shih SC, Mullen A, Abrams K, Mukhopadhyay D, Claffey KP. (1999). Role of protein kinase C isoforms in phorbol ester-induced vascular endothelial growth factor expression in human glioblastoma cells. *J Biol Chem* **274**: 15407–15414.

Sobue S, Hagiwara K, Banno Y, Tamiya-Koizumi K, Suzuki M, Takagi A *et al.* (2005). Transcription factor specificity protein 1 (Sp1) is the main regulator of nerve growth factor-induced sphingosine kinase 1 gene expression of the rat pheochromocytoma cell line, PC12. *J Neurochem* **95**: 940–949.

Sobue S, Iwasaki T, Sugisaki C, Nagata K, Kikuchi R, Murakami M *et al.* (2006). Quantitative RT–PCR analysis of sphingolipid metabolic enzymes in acute leukemia and myelodysplastic syndromes. *Leukemia* **20**: 2042–2046.

Stoeckle MY, Hanafusa H. (1989). Processing of 9E3 mRNA and regulation of its stability in normal and Rous sarcoma virus-transformed cells. *Mol Cell Biol* **9**: 4738–4745.

Stofega MR, Yu CL, Wu J, Jove R. (1997). Activation of extracellular signal-regulated kinase (ERK) by mitogenic stimuli is repressed in v-Src-transformed cells. *Cell Growth Differ* **8**: 113–119.

Taha TA, Hannun YA, Obeid LM. (2006). Sphingosine kinase: biochemical and cellular regulation and role in disease. *J Biochem Mol Biol* **39**: 113–131.

Tezuka K, Denhardt DT, Rodan GA, Harada S. (1996). Stimulation of mouse osteopontin promoter by v-Src is mediated by a CCAAT box-binding factor. *J Biol Chem* **271**: 22713–22717.

Turkson J, Bowman T, Adnane J, Zhang Y, Djeu JY, Sekharam M *et al.* (1999). Requirement for Ras/Rac1-mediated p38 and c-Jun N-terminal kinase signaling in Stat3 transcriptional activity induced by the Src oncoprotein. *Mol Cell Biol* **19**: 7519–7528.

Vlasova IA, McNabb J, Raghavan A, Reilly C, Williams DA, Bohjanen KA *et al.* (2005). Coordinate stabilization of growth-regulatory transcripts in T cell malignancies. *Genomics* **86**: 159–171.

Wilson GM, Lu J, Sutphen K, Sun Y, Huynh Y, Brewer G. (2003). Regulation of A + U-rich element-directed mRNA turnover involving reversible phosphorylation of AUF1. *J Biol Chem* **278**: 33029–33038.

Wilusz CJ, Wormington M, Peltz SW. (2001). The cap-to-tail guide to mRNA turnover. *Nat Rev Mol Cell Biol* **2**: 237–246.

Xia P, Gamble JR, Wang L, Pitson SM, Moretti PA, Wattenberg BW *et al.* (2000). An oncogenic role of sphingosine kinase. *Curr Biol* **10**: 1527–1530.

Xie W, Herschman HR. (1995). v-src induces prostaglandin synthase 2 gene expression by activation of the c-Jun N-terminal kinase and the c-Jun transcription factor. *J Biol Chem* **270**: 27622–27628.

Supplementary Information accompanies the paper on the Oncogene website (http://www.nature.com/onc)

Human Flt3 Is Expressed at the Hematopoietic Stem Cell and the Granulocyte/Macrophage Progenitor Stages to Maintain Cell Survival[1]

Yoshikane Kikushige,*† Goichi Yoshimoto,*† Toshihiro Miyamoto,† Tadafumi Iino,†§ Yasuo Mori,*† Hiromi Iwasaki,† Hiroaki Niiro,† Katsuto Takenaka,* Koji Nagafuji,* Mine Harada,* Fumihiko Ishikawa,‡ and Koichi Akashi[2]*†§

FLT3/FLK2, a member of the receptor tyrosine kinase family, plays a critical role in maintenance of hematopoietic homeostasis, and the constitutively active form of the FLT3 mutation is one of the most common genetic abnormalities in acute myelogenous leukemia. In murine hematopoiesis, Flt3 is not expressed in self-renewing hematopoietic stem cells, but its expression is restricted to the multipotent and the lymphoid progenitor stages at which cells are incapable of self-renewal. We extensively analyzed the expression of Flt3 in human (h) hematopoiesis. Strikingly, in both the bone marrow and the cord blood, the human hematopoietic stem cell population capable of long-term reconstitution in xenogeneic hosts uniformly expressed Flt3. Furthermore, human Flt3 is expressed not only in early lymphoid progenitors, but also in progenitors continuously along the granulocyte/macrophage pathway, including the common myeloid progenitor and the granulocyte/macrophage progenitor. We further found that human Flt3 signaling prevents stem and progenitors from spontaneous apoptotic cell death at least through up-regulating Mcl-1, an indispensable survival factor for hematopoiesis. Thus, the distribution of Flt3 expression is considerably different in human and mouse hematopoiesis, and human FLT3 signaling might play an important role in cell survival, especially at stem and progenitor cells that are critical cellular targets for acute myelogenous leukemia transformation. *The Journal of Immunology*, 2008, 180: 7358–7367.

Hematopoiesis is one of the most intensely studied stem cell systems where hematopoietic stem cells (HSCs)[3] self-renew, generate a variety of lineage-restricted progenitors, and continuously supply all types of mature blood cells. The technical advances of the multicolor FACS and the use of mAbs have enabled the prospective isolation of hematopoietic stem and progenitor cells according to the surface marker expression. In mice, multipotent hematopoietic activity resides in a small fraction of bone marrow (BM) cells lacking the expression of lineage-associated surface marker (Lin) but expressing high levels of Sca-1 and c-Kit (1, 2). Within the c-Kit$^+$Lin$^-$Sca-1$^+$ (KLS) fraction, the most primitive self-renewing HSCs with long-term reconstituting activity (LT-HSCs) do not express murine (m) CD34, but they do express mCD38 and a low level of mCD90 (Thy1), whereas mCD34$^+$, mCD38$^-$, or mThy1$^-$ KLS cells are short-term HSCs (ST-HSCs) or multipotent progenitors that do not self-renew (3–5). Downstream of the mCD34$^+$ ST-HSC stage, common lymphoid progenitors (CLPs) (6) and common myeloid progenitors (CMPs) (7) that can differentiate into all lymphoid cells and myelo-erythroid cells, respectively, have been purified. CMPs differentiate into granulocyte/macrophage progenitors (GMPs) and megakaryocyte/erythrocyte progenitors (MEPs), both of which are also prospectively isolatable by FACS (7).

Interestingly, the expression pattern of these surface markers in early stem and progenitor populations are considerably different in human (h) hematopoiesis. In humans, LT-HSCs express hCD34 (8). The hLT-HSC resides in the hCD34$^+$hCD38$^-$ (9, 10) or the hCD34$^+$hCD90$^+$ (11–13) fractions in both human BM and cord blood (CB). It is still unclear what percent of hCD34$^+$hCD38$^-$ or hCD34$^+$hCD90$^+$ cells are LT-HSCs in human hematopoiesis. The human counterpart for mCMPs, mGMPs, mMEPs, or mCLPs is also isolatable in the BM and the CB within the hCD34$^+$hCD38$^+$ progenitor fraction (14, 15). It has thus been suggested that, despite the difference in the expression patterns of key Ags in human and mouse hematopoiesis, lineage commitment processes from HSCs to mature blood cells might be generally preserved in both species. For example, the existence of prospectively isolatable CMPs and CLPs suggests that lineage commitment from HSCs involves myeloid vs lymphoid bifurcation in both mouse and human.

Recently, two independent groups have reported that in murine hematopoiesis, Flt3/Flk2, a tyrosine kinase receptor, is expressed in ST-HSCs but not in LT-HSCs. One group showed that mCD34$^-$

*Medicine and Biosystemic Science, and †Center for Cellular and Molecular Medicine, Kyushu University Graduate School of Medical Sciences, Fukuoka, and ‡Research Unit for Human Disease Model, RIKEN Center for Allergy and Immunology, Kanagawa, Japan; and §Department of Cancer Immunology and AIDS Dana-Farber Cancer Institute, Harvard Medical School, Boston, MA 02115

Received for publication November 26, 2007. Accepted for publication March 25, 2008.

The costs of publication of this article were defrayed in part by the payment of page charges. This article must therefore be hereby marked *advertisement* in accordance with 18 U.S.C. Section 1734 solely to indicate this fact.

[1] This work was supported in part by a Grant-in-Aid from the Ministry of Education, Culture, Sports, Science and Technology in Japan (19659248 to T.M., and 17109010 and 17047029 to K.A.) and the Mochida Memorial Foundation for Medical and Pharmaceutical Research (to T.M.).

[2] Address correspondence and reprint requests to Dr. Koichi Akashi, Medicine and Biosystemic Science, Kyushu University Graduate School of Medical Sciences, 3-1-1 Maidashi, Higashi-ku, Fukuoka, Japan. E-mail address: akashi@med.kyushu-u.ac.jp

[3] Abbreviations used in this paper: HSC, hematopoietic stem cell; AML, acute myelogenous leukemia; BM, bone marrow; KLS, c-Kit$^+$Lin$^-$Sca-1$^+$; LT-HSC, HSC with long-term reconstituting activity; ST-HSC, short-term HCS; m, murine; h, human; CLP, common lymphoid progenitor; CMP, common myeloid progenitor; GM, granulocyte/macrophage; GMP, GM progenitor; MEP, megakaryocyte/erythrocyte progenitor; CB, cord blood; MegE, megakaryocyte/erythrocyte; FL, Flt3 ligand; PI, propidium iodide; SCF, stem cell factor; Tpo, thrombopoietin; Epo, erythropoietin; CFU-GEMM, CFU-granulocyte/erythroid/macrophage/megakaryocyte; RTK, receptor tyrosine kinase; ITD, internal tandem duplication.

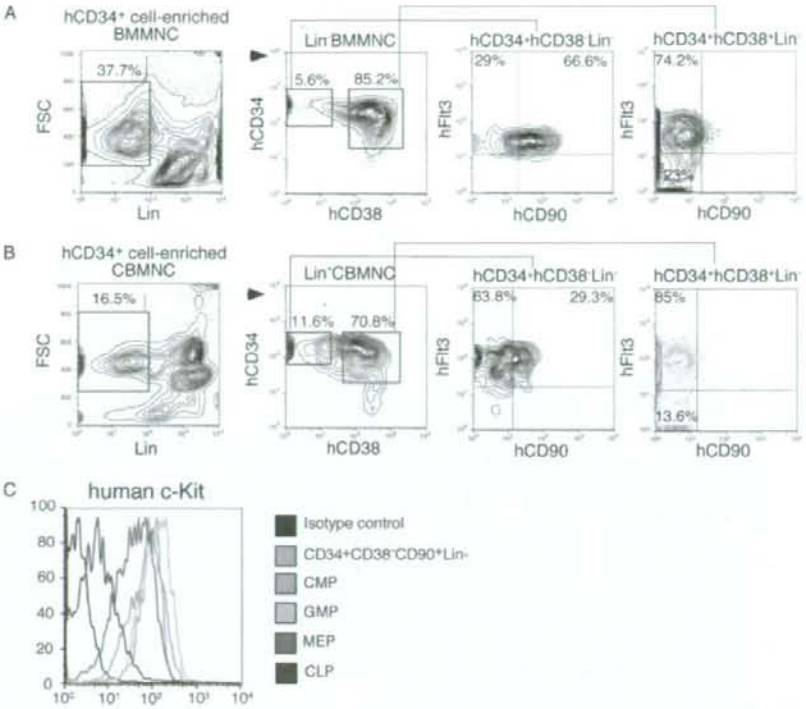

FIGURE 1. A flow cytometric analyses of human early hematopoietic populations in the BM and the CB. In $hCD34^+hCD38^-$ immature BM (*A*) and CB (*B*) cells, hFlt3 was expressed at a low level in both hCD90 (Thy1) positive and negative fractions. In contrast, the $hCD34^+hCD38^+$ BM and CB progenitor populations did not express hCD90, and hFlt3 was expressed in only a fraction of these populations. *C*, hHSCs and myeloid progenitors expressed c-Kit at high levels, and CLPs at a low level. Representative data of independent five experiments are shown here.

KLS cells (LT-HSCs) are $mFlt3^-$ (16), and the other showed that only the $mFlt3^-$ fraction of $mCD90^{low}$ KLS cells possesses LT-HSC activity (17). Each group further studied the detailed differentiation activity of $mFlt3^+$ KLS cells, but drew different conclusions. Adolfsson et al. (18) reported that the $mFlt3^+mCD34^+$ KLS population maintains the granulocyte/macrophage (GM) and the T/B lymphoid, but not the megakaryocyte/erythrocyte (MegE) potential, if any. This result suggests that, in addition to the lymphoid vs myeloid developmental pathway represented by CLPs and CMPs, respectively, there is a critical stage common to GM, T, and B lymphoid cells. The other group, however, showed that $mFlt3^+mCD90^-$ KLS cells are multipotent, thus claiming that the stage common to GM/lymphoid lineages proposed by Adolfsson et al. (18) does not constitute a major pathway for hematopoietic development (19). In contrast, downstream of the mST-HSC stage, there is a general agreement that mFlt3 is expressed in progenitors with lymphoid potential, such as the majority of CLPs and a minor fraction of CMPs, that retain a weak B cell potential (20), whereas it is down-regulated in late myeloid stages, such as GMPs and MEPs (20, 21). The Flt3 ligand (FL) is required for development of CLPs from $mFlt3^+$ KLS cells, whereas mFlt3 is dispensable for HSC maintenance and myeloid development (22). These results suggest that in mouse hematopoiesis, Flt3 signaling plays an important role in lymphoid, but not in HSC or myeloid, development.

The precise expression and the role of hFlt3 in human hematopoiesis, however, remain unclear. Around 40–80% of $hCD34^+$ BM and CB cells express hFlt3 (23, 24). Although a fraction of both the $hFlt3^+$ and the $hFlt3^-$ populations gave rise to multilineage "mixed" colonies containing all myelo-erythroid components, the $hFlt3^+hCD34^+$ and $hFlt3^-hCD34^+$ populations predominantly formed GM and erythroid colonies, respectively (23–25). It has also been shown that cells with NOD/SCID reconstitution activity reside in the $hCD34^+hFlt3^+$ fraction (24). These data collectively suggest that LT-HSCs and GMPs may reside mainly in the $hFlt3^+hCD34^+$ fraction, whereas MEPs may be contained in the $hFlt3^-hCD34^+$ fraction. Therefore, the expression pattern of Flt3 could be quite different in mouse and human hematopoiesis. Flt3 expression has also been implicated in development of human acute myelogeneous leukemia (AML). Flt3 is expressed in leukemic blasts in most cases with AML (26, 27). Furthermore, *FLT3* is one of the most frequently mutated genes in AML (28, 29), and the FLT3 mutants transduce the constitutively active FLT3 signaling, that could be the cause of poor prognosis in AML with *FLT3* mutations (30–32).

In this study, we extensively analyzed the expression and function of hFlt3 in steady-state human BM and CB hematopoiesis. Interestingly, hFlt3 was expressed in the entire human BM and CB HSC population, and purified $hFlt3^+$ HSCs could reconstitute multilineage cells for a long-term in our xenogeneic transplantation system (33). Therefore, unlike mouse hematopoiesis, the negative expression of Flt3 does not mark LT-HSCs in human. Furthermore, in striking contrast to mouse hematopoiesis where mFlt3 is expressed in CLPs but not GMPs (20, 21), hFlt3 was expressed in GMPs as well as in CLPs at a high level. The hFlt3 signaling did not affect the lineage fate decision of hHSCs, but supported cell survival of $hFlt3^+$ stem and progenitor cells, at least through the up-regulation of Mcl-1, a survival promoting Bcl-2 homologue (34). These data collectively suggest that Flt3 signaling plays a critical role in maintenance of self-renewing LT-HSCs, and of GM and lymphoid progenitors in human hematopoiesis.

Materials and Methods

BM and CB samples

Fresh human steady-state BM and CB samples were collected from healthy adults and newborns after normal deliveries. Informed consent was obtained from all subjects. The Institutional Review Board of each institution participating in this project approved all research on human subjects.

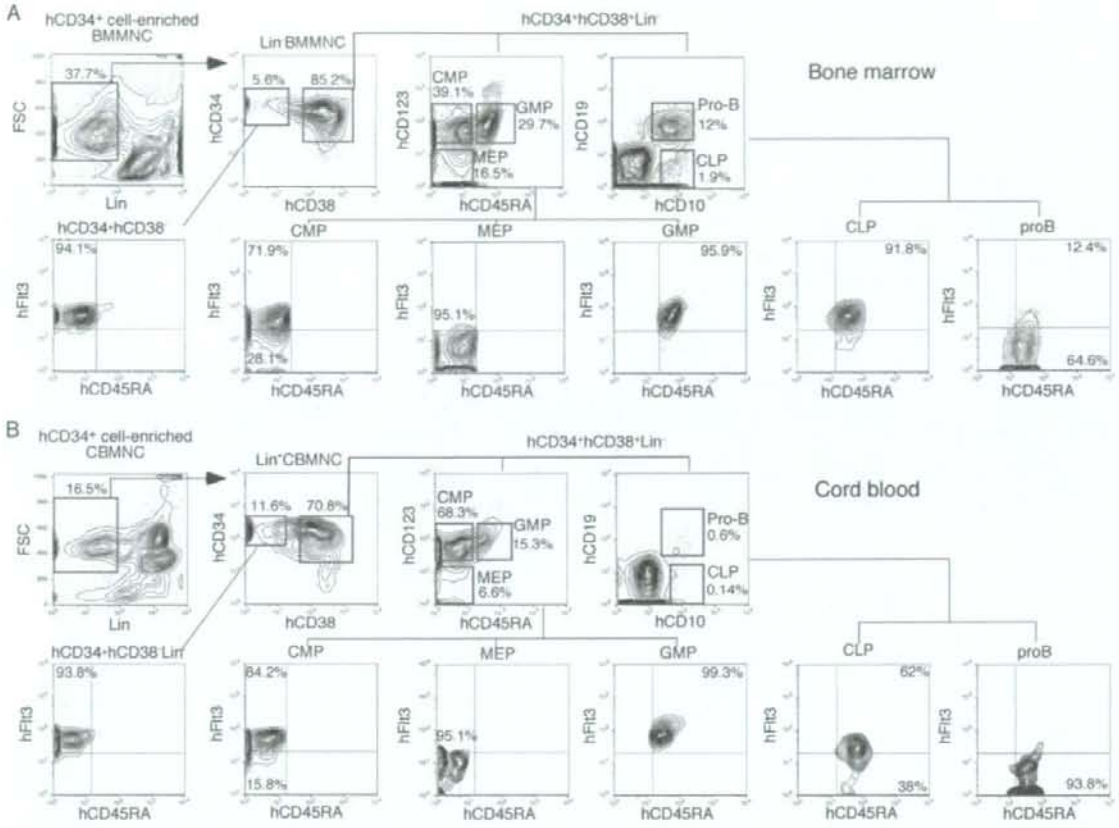

FIGURE 2. The expression patterns of hFlt3 are similar in early human BM (*A*) and CB (*B*) hematopoiesis. In the myeloid pathway in both the BM and CB, hFlt3 was up-regulated into the GM pathway, but was down-regulated in the MegE pathway; GMPs expressed hFlt3 at a high level, whereas MEPs did not express hFlt3. CMPs contained both $hFlt3^+$ and $hFlt3^-$ fractions. In the lymphoid pathway, CLPs expressed hFlt3 at a high level in BM (*A*) and a low level in CB (*B*), whereas $hCD10^+hCD19^+$ proB cells did not express hFlt3 in either the BM or the CB. Representative data of independent five experiments are shown here.

Cell preparation, flow cytometric analysis, and cell sorting

The BM and CB mononuclear cells were prepared by gradient centrifugation and the $CD34^+$ cells were enriched from mononuclear cells by using the Indirect CD34 MicroBead kit (Miltenyi Biotec) as described previously (14). For the analyses and sorting of myeloid progenitors, cells were stained with a Cy5-PE- or PC5-conjugated lineage mixture, including anti-hCD3 (HIT3a), hCD4 (RPA-T4), hCD7, hCD8 (RPA-T8), hCD10 (HI10a), hCD19 (HIB19), hCD20 (2H7), hCD11b (ICFR44), hCD14 (RMO52), hCD56 (NKH-1), and hGPA (GA-R2), FITC-conjugated anti-hCD34 (8G12), or anti-hCD45RA (HI100), PE-conjugated anti-hFlt3 (CD135) (4G8), or anti-hCD123 (6H6), allophycocyanin-conjugated anti-hCD34 (8G12), or anti-hCD38 (HIT2), Pacific Blue-conjugated anti-hCD45RA (HI100), and biotinylated anti-hCD38 (HIT2), or anti-hCD123 (9F5). The lymphoid progenitors were stained with the same lineage mixture except for the omission of anti-hCD10 and hCD19 followed by FITC-conjugated anti-hCD10 (SS2/36), PE-Cy7-conjugated anti-hCD19 (SJ25C1), and anti-hFlt3, hCD34, hCD38, and hCD45RA as described above. For additional analyses, PE-Cy7-conjugated anti-hCD34 (8G12), FITC-conjugated anti-hCD90 (5E10), PE-conjugated anti- hCD117 (YB5.B8), biotinylated anti-hFlt3 (BV10A4H2), and PE-conjugated anti-hCD127 (R34.34) mAbs were used. Streptavidin-conjugated allophycocyanin-Cy7 or PE-Cy7 was used for visualization of the biotinylated Abs (BD Pharmingen). The dead cells were excluded by propidium iodide (PI) staining. Appropriate isotype-matched, irrelevant control mAbs were used to determine the level of background staining. The cells were sorted and analyzed by FACS Aria (BD Biosciences). The sorted cells were subjected to an additional round of sorting using the same gate to eliminate contaminating cells and doublets. For single-cell assays, the re-sort was performed by using an automatic cell-deposition unit system (BD Biosciences).

In vitro assays to determine the differentiation potential of progenitors

Clonogenic CFU assays were performed using a methylcellulose culture system that was set up to detect all possible outcomes of myeloid differentiation as reported previously (14, 35). For myeloid colony formation, cells were cultured in IMDM-based methylcellulose medium (Methocult H4100; StemCell Technologies) supplemented with 20% FCS, 1% BSA, 2 mM L-glutamine, 50 μM 2-ME, and antibiotics in the presence of human cytokines such as IL-3 (20 ng/ml), stem cell factor (SCF) (20 ng/ml), FL (20 ng/ml), IL-11 (10 ng/ml), thrombopoietin (Tpo) (50 ng/ml), erythropoietin (Epo) (4 U/ml), and GM-CSF (50 ng/ml). All cytokines were obtained from R&D Systems. Colony numbers were enumerated on day 14 of culture. For the short-term liquid cell culture, cells were cultured in IMDM with 10% FCS in the presence of the cytokines described above. All of the cultures were incubated at 37°C in a humidified chamber under 5% CO_2.

Apoptosis assay and cytokine stimulation assays in the serum-free medium

To exclude the unexpected effects of FCS and to evaluate the effects of cytokine stimulation precisely, the cells were prepared in the FCS-free condition. The anti-apoptotic effect of FL and SCF was evaluated after 24 h

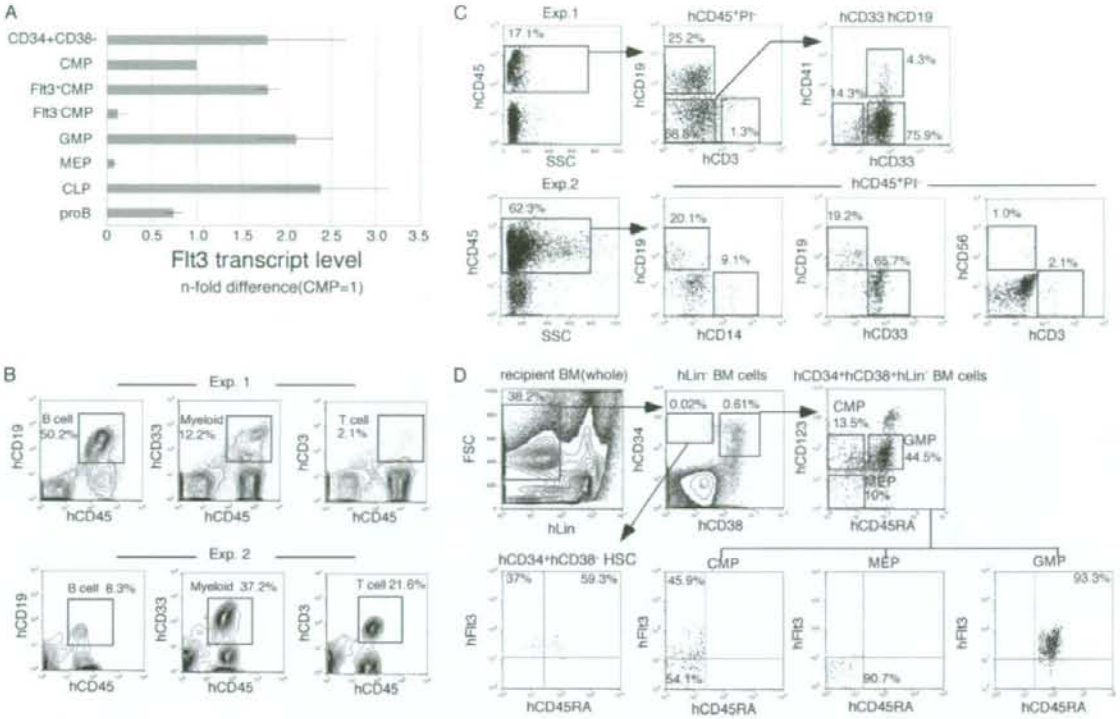

FIGURE 3. Long-term reconstitution potential of hFlt3$^+$hCD34$^+$hCD38$^-$hCD90$^+$Lin$^-$ cells in NOD/SCID/IL2rγ^{null} newborn mice. *A*, Analyses of the relative expression levels of hFlt3 transcript by real-time PCR. Each bar shows the *n*-fold difference of the level of hFlt3 mRNA in comparison to that of the whole CMP. The mean value and SD of BM samples from three independent normal donors are shown. Note that the levels of hFlt3 transcripts are well correlated with those of surface hFlt3 expression determined by FACS (Fig. 2*A*). *B*, The long-term and multilineage reconstitution of human cells in mice injected with 1×10^3 hFlt3$^+$hCD34$^+$hCD38$^-$Lin$^-$ CB cells 4 (*upper panels*) or 6 (*lower panels*) mo after transplantation. Representative two results out of five experiments are shown. *C*, Multilineage reconstitution 6 (*upper panels*) and 15 wk (*lower panels*) after i.v. injection of 5×10^3 hFlt3$^+$hCD34$^+$hCD38$^-$hCD90$^+$Lin$^-$ BM HSCs into NOD/SCID/IL2rγ^{null} newborns. Donor-derived viable human cells were evaluated as hCD45$^+$PI$^-$ cells. hCD33$^+$ granulocytes, hCD14$^+$ monocytes, hCD41$^+$ megakaryocytes, hCD19$^+$ B cells, hCD3$^+$ T cells, and hCD56$^+$ NK cells were detected in the BM of recipient mice. *D*, Stem and progenitor analyses of BM from mice reconstituted with hFlt3$^+$ HSCs. The BM contained hFlt3$^+$hCD34$^+$hCD38$^-$ HSCs, and all types of myeloid progenitors within the hCD34$^+$hCD38$^+$ population, including hCD45RA$^-$hCD123^{low} CMPs, hCD45RA$^+$hCD123^{low} GMPs, and hCD45RA$^-$hCD123$^-$ MEPs. The expression patterns of hFlt3 in each population were identical with those of freshly isolated stem and progenitor cells. A representative experiment by using BM samples from three independent normal donors is shown.

serum-free liquid culture, using Annexin V and PI staining (BD Pharmingen). The sorted cells were cultured in the serum-free medium (STEMPRO-34 SFM; Invitrogen) with or without FL (20 ng/ml) and/or SCF (20 ng/ml) for 24 h. The living cells were defined as Annexin V$^-$/PI$^-$ among the live-gated cells (as shown in Fig. 5*B*). For the cytokine stimulation assays, cells were sorted in the IMDM and then the cytokines were added.

In vivo assays to determine the differentiation potential and reconstitution capacity

The NOD.Cg-Prkdc^{scid}IL-2rg^{tm1Wjl}/Sz (NOD/SCID/IL2rγ^{null}) mice were developed at The Jackson Laboratory. The NOD/SCID/IL2rγ^{null} strain was established by backcrossing a complete null mutation at γc locus (36) onto the NOD.Cg-Prkdc^{scid} strain. The establishment of this mouse line has been reported elsewhere (37). For the reconstitution assays, the sorted cells were transplanted into irradiated (100cGy) NOD/SCID/IL2rγ^{null} newborns via a facial vein within 48 h of birth. To confirm the long-term reconstitution by hHSCs, the chimerism of circulating human blood cells were analyzed until at least 24 wk after transplantation, as previously reported (33). In addition to the Abs described above, the following mAbs were used: allophycocyanin-conjugated anti-hCD45 (J33), PE-Cy7-conjugated anti-hCD123 (6H6), FITC-conjugated anti-hCD33 (HIM3–4) or hCD14 (M5E2), and PE-conjugated anti-hCD41 (VIPL3), hCD56 (B159), anti-hGlycophorin A (GPA) (GA-R2), or anti-hCD3 (HIT3a).

Quantitative real-time PCR

To examine the gene expression profile of each population, RNA was isolated from 2,000-sorted cells using Isogen reagent (Nippon gene) according to the manufacturer's instructions. The total RNA was reverse transcribed to cDNA using a TaKaRa RNA PCR kit (Takara Shuzo). The mRNA levels were quantified in triplicate using a real-time PCR (7500 Real-Time PCR system; Applied Biosystems). hβ2-microglobulin mRNA was separately amplified in the same plate to be used for internal control. The primer and probes were designed by Primer Express software (Applied Biosystems).

Results

The hCD34$^+$hCD38$^-$ HSC fraction express hFlt3 at a low level in both BM and CB

The hCD34$^+$Lin$^-$ population was divided into hCD38$^+$ and hCD38$^-$ populations (Fig. 1, *A* and *B*). It has been shown that HSCs with long-term reconstitution activity reside in the hCD38$^-$ fraction within the hCD34$^+$ BM and CB populations (9, 10). As shown in Fig. 1*A*, in the BM, hCD38$^-$ cells constituted only ~5% of the Lin$^-$hCD34$^+$ population. This population uniformly expressed hFlt3 at a low level. More than

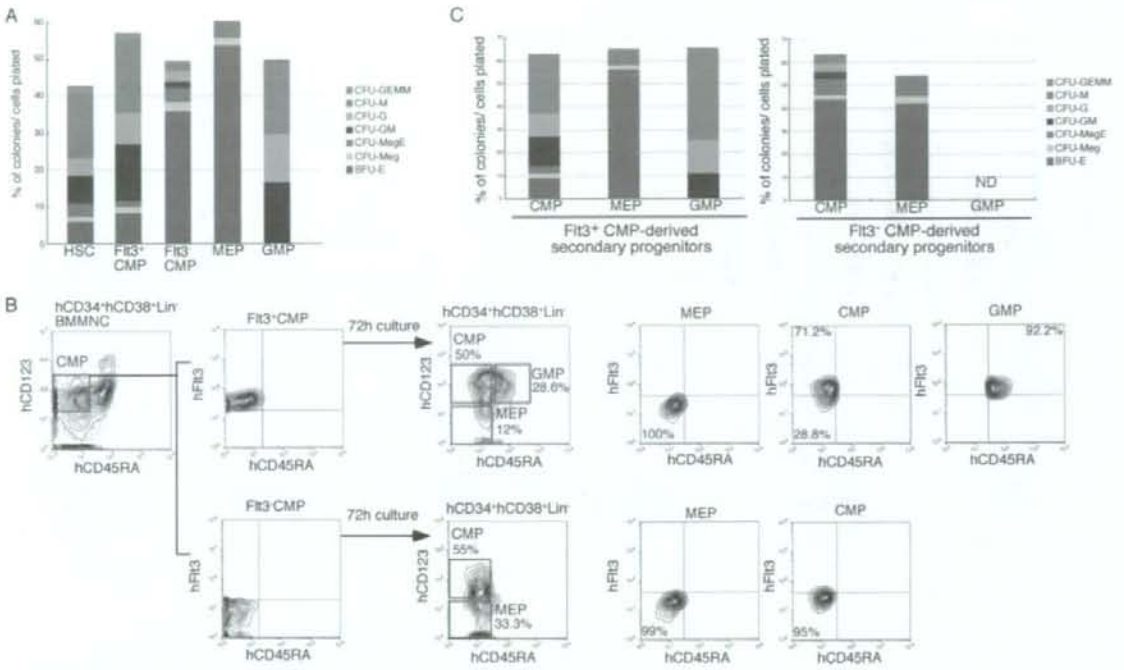

FIGURE 4. The lineage potential and the relationship of myeloid progenitor populations. *A*, Clonogenic colony formation of purified populations on methylcellulose in the presence of cytokine mixture. The hCD34$^+$hCD38$^-$ HSCs and hFlt3$^+$CMPs gave rise to various myeloid colonies including CFU-GEMM, whereas GMPs and MEPs formed exclusively GM and MegE lineage-related colonies, respectively. In contrast, hFlt3$^-$CMPs predominantly gave rise to MegE lineage-related colonies but failed to form CFU-GEMM. The mean value of eight independent experiments is shown. CFU-M: CFU-macrophage, CFU-G: CFU-granulocyte, CFU-GM: CFU-granulocyte/macrophage, CFU-MegE: CFU-megakaryocyte/erythroid, CFU-Meg: CFU-megakaryocyte, and BFU-E: burst-forming units-erythroid. *B*, The lineal relationship between hFlt3$^+$CMPs and hFlt3$^-$CMPs. After 72 h of culturing, hFlt3$^+$CMPs gave rise to hFlt3$^-$CMPs, GMPs, and MEPs. In contrast, hFlt3$^-$CMPs differentiated into only MEPs, thus suggesting hFlt3$^-$CMP to be a transitional intermediate population from hFlt3$^+$CMPs to hFlt3$^-$MEPs. *C*, The colony formation activity of phenotypically defined secondary CMPs, GMPs, and MEPs purified from the primary culture of hFlt3$^+$CMPs or hFlt3$^-$CMPs. Each population displayed the colony formation activity consistent with their phenotypic definition. The mean value of four independent experiments is shown.

60% of the hCD34$^+$hCD38$^-$ BM cells also expressed hCD90, another critical marker for hHSCs (11–13), whereas the hCD34$^+$hCD38$^+$Lin$^-$ fraction was constituted of hCD90$^-$ lineage-committed progenitors.

In the CB, only ~30% of hCD34$^+$hCD38$^-$ cells expressed hCD90 (Fig. 1*B*). In the NOD/SCID/IL2rγ^{null} newborn system, the hCD34$^+$hCD38$^-$hCD90$^+$ population was highly enriched for HSCs capable of long-term reconstitution as compared with the hCD34$^+$hCD38$^-$hCD90$^-$ CB fraction (F. Ishikawa, unpublished data). The vast majority of hCD34$^+$hCD38$^-$ cells expressed hFlt3 at a low level as previously reported (38). Furthermore, the hCD34$^+$hCD38$^-$hCD90$^+$ CB population expressed hFlt3.

These data clearly show that hFlt3 is expressed in all cells with the hHSC phenotype in both the BM and the CB, and suggest that Flt3 expression does not discriminate ST-HSCs from LT-HSCs in human as it does in mouse (16, 17). In contrast, the BM and the CB hCD34$^+$hCD38$^+$ progenitor fraction expressed negative to high levels of hFlt3. We thus further subfractionated the hCD34$^+$hCD38$^+$ population to evaluate the hFlt3 expression in a variety of lineage-restricted progenitors.

The expression of hFlt3 within the hCD34$^+$hCD38$^+$ progenitor fraction

In mouse hematopoiesis, the expression of mFlt3 is associated with early lymphoid progenitor activities; it is expressed in the majority of CLPs, and in the minority of CMPs with weak B cell potential (20), but not in MEPs or GMPs (20) (21). Fig. 2 shows the expression of hFlt3 in the myeloid and lymphoid progenitor populations. According to the phenotypic definition of human myeloid and lymphoid progenitors (14, 15, 39, 40), hCD34$^+$hCD38$^+$ cells were subfractionated into myeloid and lymphoid progenitors, including the hCD45RA$^-$hCD123 (IL-3Rα)^{low} CMP, the hCD45RA$^-$hCD123$^-$ MEP, the hCD45RA$^+$hCD123^{low} GMP, the hCD10$^+$hCD19$^-$ CLP, and the hCD10$^+$hCD19$^+$proB populations. Interestingly, in both the human BM and CB, ~70–80% of CMPs expressed hFlt3, whose level was progressively up-regulated at the GMP stage. In contrast, hFlt3 expression was completely shut down in MEPs. In the lymphoid lineage, the hCD34$^+$hCD38$^+$hCD10$^+$ CLP (15) strongly expressed hFlt3, whereas hFlt3 was down-regulated in the proB cells. The expression level of hFlt3 in GMPs and CLPs appears to be higher than that in hCD34$^+$hCD38$^-$hCD90$^+$ HSCs (Fig. 2). We also tested the level of hFlt3 transcripts in purified hBM HSCs and progenitor populations (Fig. 3*A*). The pattern of hFlt3 mRNA expression was generally consistent with that in hFlt3 protein, as evaluated by using anti-hFlt3 Abs on FACS (Figs. 1 and 2). Consistent with a previous report (41), MEPs and hFlt3$^-$ CMPs had the lowest levels, GMPs and CLPs had the highest levels, and the hCD34$^+$hCD38$^-$ HSC population had a medium level of hFlt3 mRNA. Collectively, functional hLT-HSCs express hFlt3 mRNA

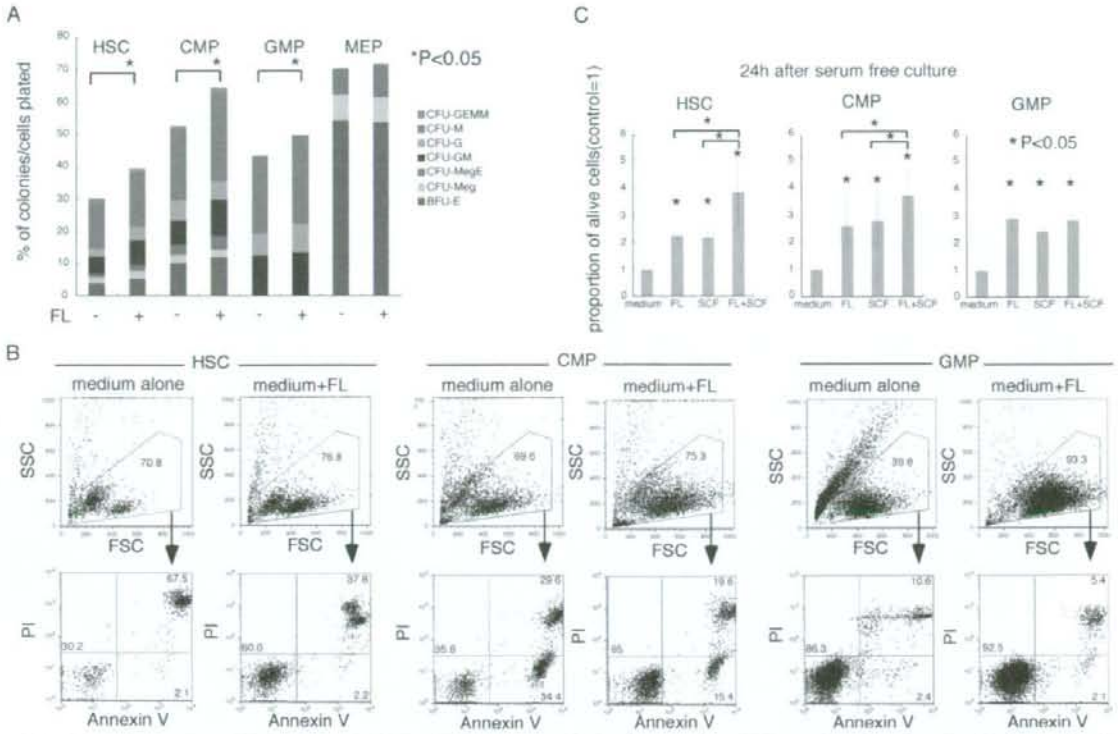

FIGURE 5. Effect of FL and SCF on the survival of purified progenitors. *A*, The effect of additional FL on colony formation of purified progenitors in methylcellulose in the presence of SCF, IL-3, IL-11, GM-CSF, Epo, and Tpo. Results from five independent experiments are shown here. Note that colony numbers are increased by the addition of FL into cultures in all hFlt3-expressing subsets including HSCs, CMPs, and GMPs but not in hFlt3$^-$ MEPs. *B*, An evaluation of apoptotic cell death in cultures of stem and progenitor cells. HSCs, hFlt3$^+$ CMPs, and GMPs were cultured in the serum-free media, with or without FL, and analyzed at 12, 18, 24, 30, 48, and 72 h after initiation of culture. A representative data obtained after 24-h culture is shown. *C*, Anti-apoptotic effects of FL and/or SCF on HSCs and Flt3$^+$ CMPs. Annexin$^-$ PI$^-$ live cells were enumerated after 24-h culture in a serum-free media. Each graph shows n-fold differences in the percentage of live cells relative to the ones without cytokine. Each bar represents the mean value and the SD of five independent samples.

and surface protein, and the distribution of Flt3 is quite different between human and mouse in early hematopoiesis.

In contrast, c-Kit was expressed at high levels in human HSCs and myelo-erythroid progenitors, while at a low level in CLPs (Fig. 1*C*). The expression pattern of c-Kit in human hematopoietic stem and progenitor cells is generally consistent with that in mouse hematopoiesis (4, 6, 7), suggesting that the c-Kit expression program is preserved in mouse and human hematopoiesis.

hFlt3 is expressed in functional hHSCs capable of reconstituting normal hematopoiesis in the NOD/SCID/IL-2 receptor γ-chain null (NOD/SCID/IL2rγ^{null}) mouse model

In the NOD/SCID/IL2rγ^{null} newborn system, hCD34$^+$hCD38$^-$ BM and CB cells are capable of reconstitution of all hematopoietic lineages for a long term (33). The entire hCD34$^+$hCD38$^-$ BM population expressed hFlt3 (Fig. 1*A*), suggesting that functional hBM HSCs possess hFlt3 on their surface. In contrast, hCD34$^+$hCD38$^-$ CB cells contained some hCD90$^-$ cells that did not express hFlt3. To formally test whether Flt3-expressing hCD34$^+$hCD38$^-$ CB cells possess LT-HSC activity, we transplanted hFlt3$^+$hCD34$^+$hCD38$^-$hCD90$^+$ CB cells in to NOD/SCID/IL2rγ^{null} newborns. As shown in Fig. 3*B*, NOD/SCID/IL2rγ^{null} mice transplanted with 1×10^3 hFlt3$^+$hCD34$^+$hCD38$^-$hCD90$^+$ CB cells reconstituted all hematolymphoid lineages for >6 mo, indicating that hFlt3 is expressed in functional hHSCs in CB as well as in BM.

Fig. 3*C* shows the phenotypic analysis of human progeny from 5×10^3 hFlt3$^+$hCD34$^+$hCD38$^-$hCD90$^+$ BM cells 6 (*upper panels*) or 15 wk (*lower panels*) after transplantation into NOD/SCID/IL2rγ^{null} newborns (33). hFlt3$^+$hCD34$^+$hCD38$^-$hCD90$^+$ BM cells differentiated into all hematopoietic lineage cells, including hCD33$^+$ granulocytes, hCD14$^+$ monocytes, hCD41$^+$ megakaryocytes, hCD19$^+$ B cells, hCD3$^+$ T cells, hCD56$^+$ NK cells (Fig. 3*C*), and hGPA$^+$ erythrocytes (not shown). Furthermore, transplanted hFlt3$^+$hCD34$^+$hCD38$^-$ HSCs purified from primary recipients developed secondary hFlt3$^+$ HSCs and hFlt3$^{-/+}$ CMPs, hFlt3$^-$ MEPs, and hFlt3$^+$ GMPs recapitulating normal human hematopoietic development. Thus, the hCD34$^+$hCD38$^-$hCD90$^+$ BM population contains cells with long-term SCID reconstitution potential as reported (33, 42), and all cells within this population express hFlt3 on their surface (Fig. 3*D*).

The up- or down-regulation of hFlt3 in the myeloid pathway is associated with GM or MegE differentiation activity, respectively

Fig. 4*A* shows the differentiation potential of purified BM progenitors in vitro in the presence of the myeloid cytokine mixture containing SCF, FL, IL-3, IL-11, Tpo, Epo, and GM-CSF. hFlt3$^+$